QATAR UNIVERSITY

COLLEGE OF ENGINEERING

FACTORS INFLUENCING THE MECHANICAL PROPERTIES OF GEOPOLYMER MORTAR MADE OF FLY ASH

BY

MOHAMED HASSAN KAMEL HASSAN RABIE

A Thesis Submitted to

the Faculty of the College of Engineering

in Partial Fulfillment of the Requirements for the Degree of

Master of Science in Civil Engineering

June 2020

COMMITTEE PAGE

The members of the Committee approve the Thesis of
Mohamed Hassan Kamel Hassan Rabie defended on 22/04/2020.

_____
Dr. Mohamed Irshidat & Dr. Nasser Alnuaimi
Thesis Supervisors

_____
Dr. Wael Alnahhal
Committee Member

_____
Dr. Faris Matalkah
Committee Member

Approved:

_____
Khalid Kamal Naji, Dean, College of Engineering

ABSTRACT

RABIE, MOHAMED, H., Masters: June : 2020,

Masters of Science in Civil Engineering

Title: FACTORS INFLUENCING THE MECHANICAL PROPERTIES OF GEOPOLYMER MORTAR MADE OF FLY ASH

Supervisors of Thesis: Dr. Mohammad R. Irshidat and Dr. Nasser Al-Nuaimi

Geopolymerization is a process where silica and alumina rich source materials turns into excellent binding materials by the aid of alkali solutions. Fly ash class F mainly consists of alumina and silica. Compressive strength of class F fly ash geopolymer mortar is influenced by many factors such as fluid to binder ratio, Na2SiO3/NaOH ratio, curing duration, curing temperatures, age of geopolymer mortar GPM and molarity of the NaOH solution. The present experimental study investigates the effect of these factors on the compressive strength of geopolymer mortar. For each combination, three cubes with dimensions of 50 x 50 x 50 mm were casted. After heat curing in the laboratory oven, the samples were tested on a universal testing machine for the compressive strength. A microstructural study was conducted to observe the internal structure using Scanning electron microscopy, Energy-dispersive X-ray spectroscopy and X-ray diffraction analysis. The results showed very high early compressive strength of 63.9 MPa for samples cured at 80 °C and for a duration of 24 hr. The significance of the present study is that it will allow for establishing methods for production of high strength geopolymer mortar that can be used in civil engineering applications. In addition to the environmental advantages of using such source materials to produce binding materials with good mechanical properties.

DEDICATION

This thesis is dedicated to my family, friends, and dear ones. There continuous support and efforts are utterly appreciated. To my supervisors, mentors and teachers your guidance and teachings will never be forgotten. Thank you!

ACKNOWLEDGMENTS

First and foremost, I would like to thank Almighty Allah for all his blessings.

I would like to express my deepest gratitude to my supervisors Dr. Mohammad Irshidat and Dr. Nasser Al-Nuaimi for their endless support and guidance through the undertaken of this work. They were always trying to push me to hone my research skills and for that I am utterly grateful.

Furthermore, I would like to thank Qatar University for their support in accessing the facilities and conducting the experimental work. Special thanks to the Center for Advanced materials and College of Engineering staff for the support and guidance. I would like to thank my friends with their initials as: K.R, A.A, M.A and M.N for always encouraging me to complete this project.

Finally, my deepest gratitude towards my lovely family and my nephews Bassem and Yousef for their support. Thanks all, for you all I will be utterly grateful!

TABLE OF CONTENTS

LIST OF TABLES

LIST OF FIGURES

NOTATION AND SYMBOLS

NaOH	Sodium hydroxide
Fc	Compressive strength
Na2Sio3	Sodium silicate
F	Fluid to binder ratio
N	Sodium silicate/sodium hydroxide ratio
GPM	Geopolymer mortar
GPC	Geopolymer concrete
OPC	Ordinary Portland cement
T	Temperature
D	Duration
FA	Fly ash
AAM	Alkali activated materials
CM	Cement mortar

CHAPTER 1: INTRODUCTION

1.1 Hypothesis and Research Problems

Cement production processes requires immense amount of energy and is accountable for 7% carbon dioxide emissions to the atmosphere. It is estimated that production of one ton of cement is equivalent to one tone of CO2 [1]–[3]. There has been an increasing demand to develop a new binding material that can partially or fully replace cement in mortar and concrete. Geopolymerization is a process where three-dimensional polymeric chain rings consisting of Si-O-Al-O are formed by alkali activating the source material that are rich with silica and alumina [4]. Binding materials prepared by the geopolymerization process has proven its competency to provide good binding materials, achieving similar or better mechanical properties than cement-based building materials [5], [6]. Activator solutions used in production of geopolymer mortar and concrete are mainly potassium and sodium alkaline solutions. The mechanical strength of geopolymer mortar are affected by many factors such as fluid to binder ratio, curing temperature, molarity of the activator solution and the ratio of the Na2SiO3 to NaOH. Similarly, the mechanical properties of cement-based mortar and concrete are highly affected by w/c ratio [4]. Recent literature has proved that fly ash is efficiently activated by sodium based alkaline activators [2]. Thus, scientists are conducting research in this particular field to establish means of using such materials in the construction industry replacing cements. Figure 1 shows the advantages of using geopolymers in the construction industry.

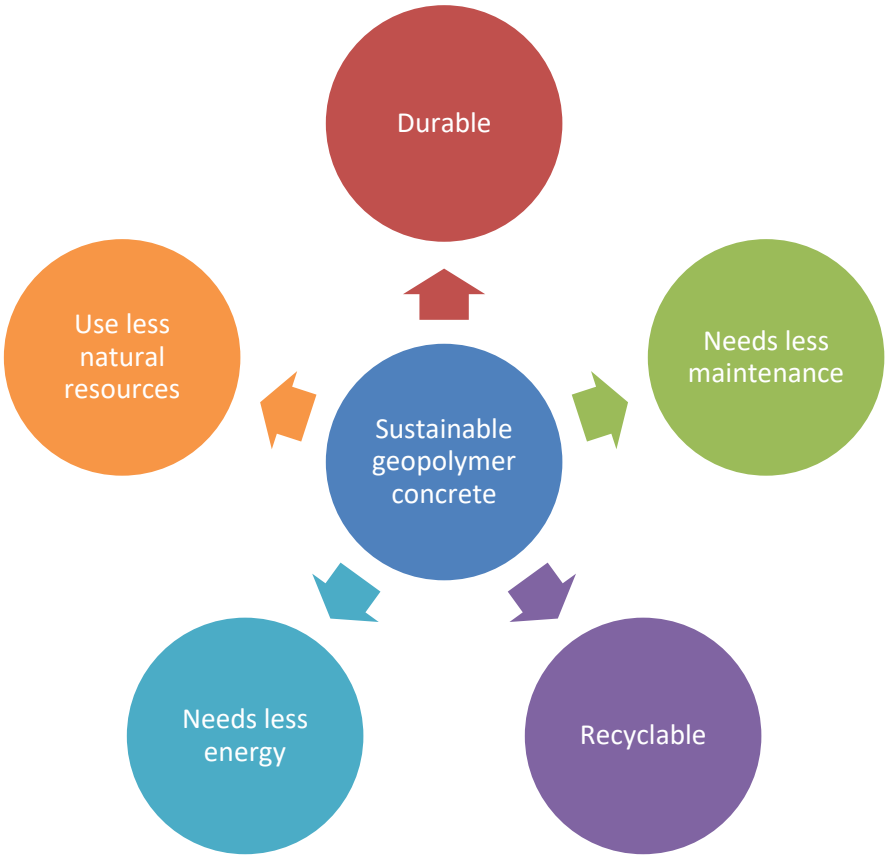

Figure 1. Research Motivation

The present research work investigates all the factors influencing the production of geopolymer mortar. Including best curing practices for the use in civil engineering applications as an innovative construction material.

1.2 Aims and Objectives of the Study

The aim of this study is to investigate the factors influencing the mechanical properties of geopolymer mortar (GPM), and what are the best practices and optimum conditions. In order to determine the casting and curing practices to produce high strength geopolymer mortar. The factors investigated in this study are:

- Molarity of the activator solution
- Activators solution to binder ratio

- Sodium hydroxide to sodium silicate ratio
- Curing temperature
- Curing duration
- Age of geopolymer mortar

The main objectives of this study are listed as follows:

- To investigate the effect of the molarity of the activator solution in the compressive strength, internal structure, rheology and development of the polycondensation products in geopolymer mortar.
- To study the best curing conditions that allows the development of high strength geopolymer mortar.
- To investigate the effect of age in the mechanical strength of geopolymer mortar.
- To produce GPM using fly ash as source material instead of cement and activated by alkaline solutions.
- To study the effect of solution to fly ash ratio and Sodium silicate/ Sodium hydroxide ratio on workability and compressive strength of GPM.
- To study the internal structure of geopolymer mortar with and without the use of sodium silicate as an activator solution.

1.3 Methodology

This research includes six test parameters; namely, (a) Molarity of the NaOH activator solution: 12, 14 and 16M, (b) Fluid to binder ratios of: 0.60, 0.65 and 0.70, (c) Sodium hydroxide to sodium silicate ratios of: 1, 1.5, 2 and 2.5, (d) Curing temperatures of: 40, 80 and 120 ^{o}C, (e) Curing durations of 24, 48 and 72 hours. (f) age of geopolymer mortar of 0, 3 7 and 28 days. The experimental program is divided into three phases. Phase one is aimed to study the first three factors (a, b and c) at fixed curing temperature and duration. The second phase is to study the curing conditions factors (d, e). The last phase is to study the effect of age on the best geopolymer mix design at different ages for samples cured with optimum curing conditions resulted from the second phase, and for ambient curing temperature. Total of 162 GPM specimen were casted to conduct the experimental program. The results were mainly investigated in terms of the compressive strength, the workability and the microstructure.

1.4 Structure of the Thesis

Chapter 2: Background and Literature Review– this chapter introduces a general background about the topic of alkali activated materials, with an up to date literature review.

Chapter 3: Experimental Program – this chapter includes the material properties, experimental matrix, specimen's description, mixing procedures, test setup, and equipment.

Chapter 4: Results and Discussion – this chapter includes the results and discussion for the experimental results and the influence of different test parameters included in this study.

Chapter 5: Conclusion and Recommendation– this chapter states the findings of the research and recommendations for future work.

CHAPTER 2: BACKGROUND AND LITERATURE REVIEW

This chapter begins with a background and introduces the topic of geopolymer as a construction material. After that, an up to date literature review is provided for the different materials used and the development of geopolymer along the history. Eventually, a summary of the literature is provided, and how the current research is related to the advancement of using geopolymers as a construction material.

2.1 Background

The first patent that introduced the idea of a reaction of an alkali solution with Al and Si source material was done by the German scientist Kuhl [7]. The formed solid material was comparable to hardened cement with a performance equal or better than the best Portland cement. The concept was further developed by Purdon [8], where he tested multiple source material activated by sodium hydroxide solutions and with different sodium salts, Purdon achieved strengths that were comparable to Portland cements. It was further noted in his studies that the improved tensile and flexural strengths of alkali activated mixes compared to Portland cement.

Davidovits was the first to apply the name of “geopolymer” to the alkali activated materials [9]. He patented multiple formulations on the reaction of geopolymer starting from 1980s. Figure 2 shows the classifications of alkali activated materials with comparison to ordinary Portland cements.

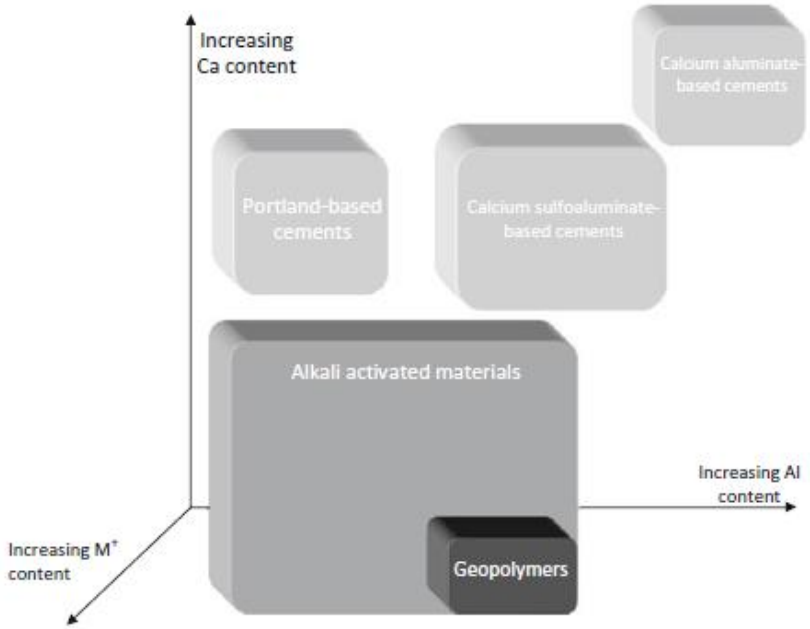

Figure 2.Classification of AAMs [10]

The second reason where scientist started looking for alternative construction materials is the environmental impact the cement production on the environment. Cement is the second used commodity directly after water, and the production of cement soared to 2.9 billion tons in 2008 [11]. This huge production volume has significant impact on the environmental, as cement production contributes to around 8% of global CO2 emissions [12]. The reason behind this enormous amount of CO2 released to the atmosphere is directly related to the processes of cement production, as it requires high temperature to decompose limestone to active aluminate and calcium silicate. The demand for cement production is growing quickly specially in the developing countries [13]. Figure 3 illustrates the processes of producing cement and how CO2 is emitted to the atmosphere in each process.

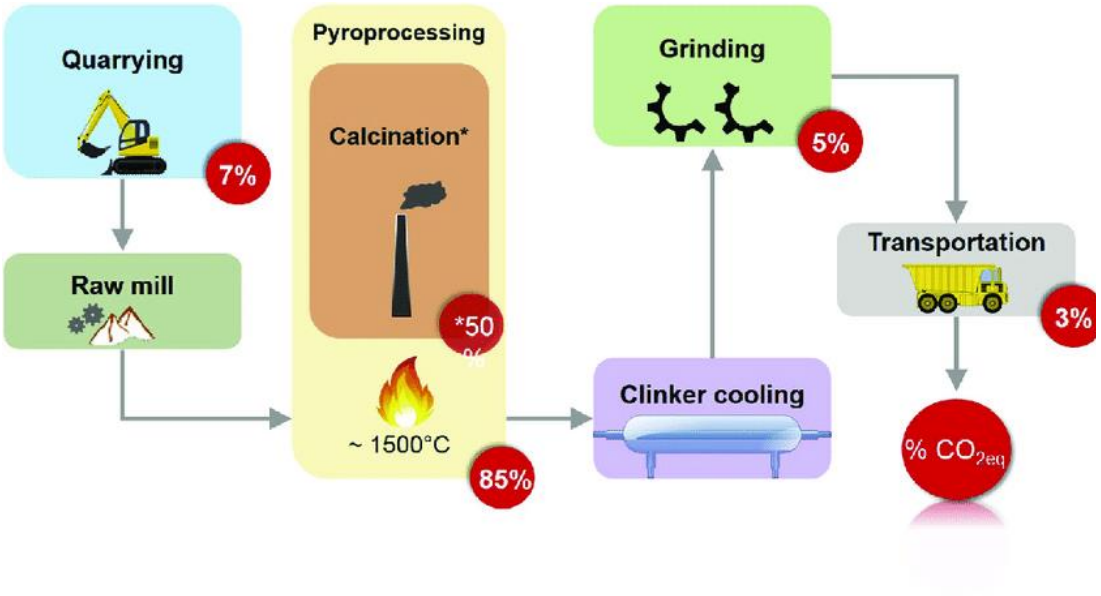

Figure 3. Production processes of cement [14]

Thus, industry leader tries to minimize the emissions of CO2 by optimizing the process of production of cement which estimated to reduce CO2 by only 17% [15]. One of the alternatives of OPC that have less environmental impact on the environment is alkali activated materials, as it has much lower emissions of CO2 associated with the production of alkali activated materials. This is mainly due to the avoidance of high temperature in the production of source materials such as fly ash [16]. Geopolymers can be produced by the dissolution of Al and Si in the source materials, such as fly ash in a strong alkaline solution. Then alumni and silicon oxides reorganize and polycondensation process occurs to transform into a hardened state. The production of geopolymers as construction materials and the factors influencing their mechanical properties are not yet well investigated in the literature.

2.2 Geopolymers

Geopolymers are inorganic materials that polycondense in a comparable way to organic polymers. The reaction of aluminate and silicate with alkali solutions produces a three-dimensional structure of polymeric sialate (Si-O-Al-O) bonds, with amorphous structure. As shown in Figure 4.

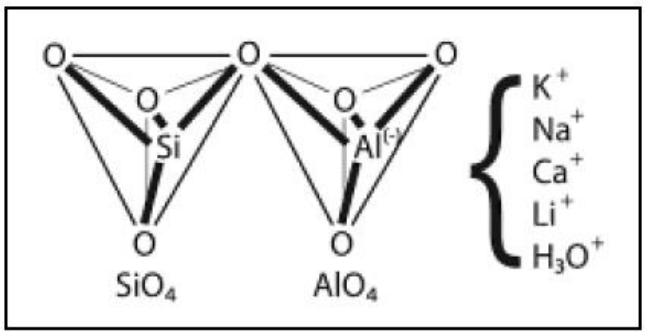

Figure 4. Tetrahedral configuration of sialate [17]

Through the reaction of hydroxide ions and the aluminate and silicate in the source material dissolves and the ions organize into monomers and then polycondense to form polymeric structures [18]. Water is released during the formation of the geopolymer matrix. On the contrary the hydration for Portland cement requires water in order for the chemical reaction to occur [18]. Figure 5 shows the polymerization model and the steps for the geopolymerization to occur.

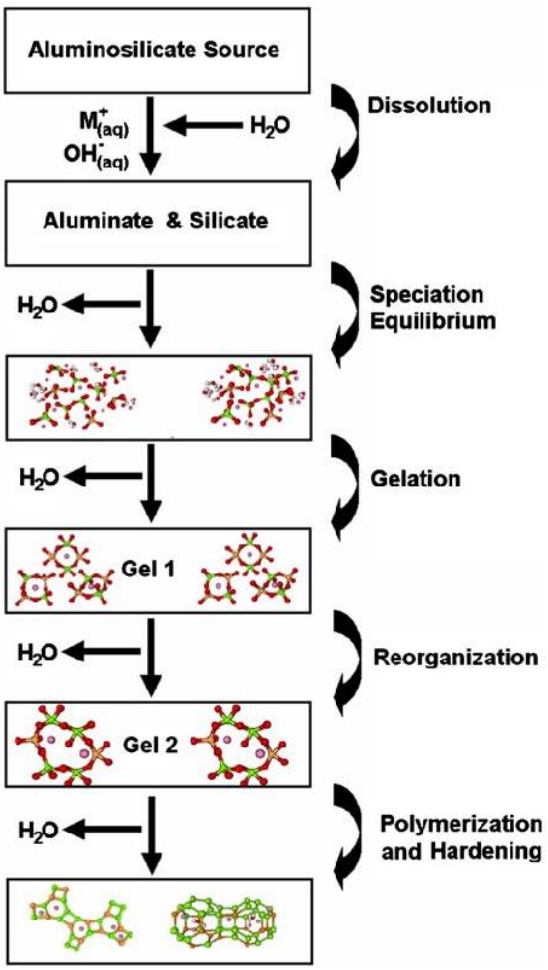

Figure 5. The polymerization process of AAM

Source material rich with aluminate and silicate can come from natural sources as kaolinite and clays, or as byproducts from manufacturing process, such as fly ash, slag and silica fume. These materials can be used in the producing geopolymers, when mixed with alkali solutions.

2.3 Fly ash

The use of fly ash as a component of cement binders is not new; fly ashes were mixed with Portland cement [19], which consisted of almost omnipresent use in today's exercise in some elements of the world (although in some other cases much more

limited, based on jurisdictional choices and near-by availability of ash). High-profile fly ash concretes, where Portland cement is blended with more than 50 percent fly ash, see more substantive applications because their special workability and healing requirements are starting to be better understood [20], Although, in the absence of a clinker, the particular case of alkaline activation involves a much more detailed know-how in fly ash glass chemistry, since this is the easiest source of reactive binder forming materials. Fly ash that is produced from bitimous coals are class F as it has large content of aluminate and silicate, but less than 10% calcium oxide (CaO). On the other hand, class C fly ash has large amounts of CaO greater than 10%, which gives it unique hardening properties. The presence aluminate and silicate in fly ash has encouraged to use it as a source material in producing geopolymers as a replacement of cement [21]–[23]. For fly ash class F the main polymerization products are Si-O-Al-O bonds. In contrast, for fly ash class C that contains both aluminate and silicate and CaO there are polymerization products produces Si-O-Al-O bonds in parallel to the C-S-H and C-A-H. The presence of CaO in fly ash class F can improve the reaction, thus improving the hardened matrix [24]–[27]. In this study fly ash class F was used to produce geopolymer mortar.

2.4 Type of activator solution

The alkali solutions are generally composed of two components, one is sodium/potassium hydroxide (NaOH/KOH) solution, and the second is sodium/potassium silicate solution (Na2SiO3/K2O3Si). The most common used alkali solutions are those of sodium ions. (Silverstrim et al., 1997) recommended that the for NaOH solution to be composed of 25-100% NaOH with up to 75% water. Further, it is recommended for sodium silicate solution to be of a concentration ranging from 38-

55% Na2SiO3 and 45-62% of water [28]. The addition of sodium silicate solution increases the minerals, which can improve the strength and it improves the hardening properties of the binder. The addition NaOH solution increases the dissolution rates in the source materials, and its exothermic characteristics, thus allowing for better formation of polymerization products [17].

An experimental study was conducted by Hardjito & Rangan (2005) to study the effect of sodium silicate and sodium hydroxide as activator solutions on the production of geopolymer concrete (GPC) [29]. NaOH solutions were prepared with molarities varying from 8M to 16M and Na2SiO3/NaOH ratios ranging from 0.4 to 2.5, naphthalene sulfonate super plasticizer was used at dosages of 0% - 2% for improved workability. The results of the experimental study suggested that the higher the concentration of sodium hydroxide solution and the higher the ratio of Na2SiO3/NaOH resulted in stronger specimens. Further, it was noted that the effect of using 2% superplasticizer on has improved the workability of GPC without affecting the compressive strength.

An experimental study was conducted by Mustafa et al. (2011) to study the production of geopolymer using class F fly ash [30]. The fly ash was acquired from a power station in Malaysia. NaOH solution with concentration of 15M and sodium silicate solution of 39.5 % Na2SiO3 and 60.5 % water. Further, the author studied the effect of fluid to binder ratio. GPM was casted in 5cm cube specimens, specimens were casted for 24 hrs. at room temperature, and then subjected to heat curing for another 24 hrs. at a temperature of 70 ^{o}C. The results showed that compressive strength was highest of 8.3 MPa after curing and an age of 7days. The low compressive strength was attributed to the curing conditions and the mixing procedures. Similar findings were reported by multiple authors [31]–[33].

Kaur et al. (2018) conducted an experimental study to study the effect of different concentrations and combinations of alkaline activators [34]. NaOH solutions were prepared at 12, 16 and 16M with sodium silicate solution of 37% concentration. The curing conditions were fixed for all specimens at 80 oC for 24 hrs. then samples were left at room temperature for ages of 3,7,14 and 28 days. The results indicated that the compressive strength increases as the concentration of sodium hydroxide solution, and the presence of sodium silicate solution significantly enhanced the compressive strength of GPM. A maximum compressive strength of 40.42 MPa was achieved by mix design that is activated by 16 M NaOH solution and sodium silicate solution.

2.5 Ambient curing Vs. Heat curing

Several studies have shown the effect of heat curing as it plays a significant role in the geopolymerization process and the mechanical properties of geopolymers [32], [35]–[39]. As the polymerization process of fly ash is very low when specimens cured at ambient temperature, and the rate of the polymerization process increases as the curing temperature increases.

Görhan et al. (2014) conducted an experimental study to study the mechanical properties of ambient cured geopolymer concrete [40]. Geopolymer concrete was activated by sodium hydroxide solution only with fluid to binder ratio at 0.35. The results showed that the compressive strength of geopolymer concrete was extremely low at ages of 7 and 28 days reaching 1 and 4 MPa, respectively.

Another study conducted by Atiş et. Al (2015) aimed to produce geopolymer mortar using class F fly ash, activated at different NaOH amounts with different heat curing temperatures and durations [41]. The compressive strength of GPM cured below 55 ^{o}C exhibited a very low compressive strength compared to GPM specimens cured above 75 ^{o}C. The maximum compressive strength reached was 120 MPa for samples cured at

115 ^{o}C and a duration of 24 hrs. This indicates the importance of heat curing in the development of geopolymerization products, which directly impact the mechanical properties of GPM. Further, the study showed that the duration of curing is also another factor affecting the compressive strength. As for longer durations of curing (72 hrs.) a low heat temperature is preferable. On the contrast, for shorter duration of curing (24 hrs.) high heating temperature is enough to obtain similar compressive strength.

Numerous studies showed the importance of heat curing in the production of geopolymer construction materials [41]–[45].

2.6 Review summary

Based on the findings reviewed from the literature about the factors influencing the production of geopolymer mortar. The summary of the findings can be stated as follows:

- The compressive strength increases by increasing the concentration of the activator solutions.
- Excessive hydroxide ions cause the binder to lose strength, as it accelerates the dissolution of the aluminate and silicate in the source materials. However, it decreases the polycondensation process.
- Water can be used to enhance the workability of geopolymer construction materials; however, excess water content can lead to segregation of the constituent's materials and ultimately reduces the strength.
- Strength increases by increasing the curing temperature of geopolymer and increases with the age.
- Activator solution to binder ratio affects the mechanical properties and the rheology of geopolymer.

- Superplasticizers can be used to improve the workability of geopolymers without impacting the mechanical properties.
- The fineness of fly ash is one of the factors the impacts the mechanical properties, as the finer the particles the increased surface area, the better the mechanical properties.
- Fly ash class C will have hydrations products of C-S-H and C-A-H along polymerization products of Si-O-Al-O, which leads to better mechanical properties than geopolymer made of fly ash class F.
- Different sodium silicate / sodium hydroxide ratios can influence the mechanical properties of geopolymer materials.

CHAPTER 3: EXPERIMENTAL PROGRAM

3.1 Material Properties

3.1.1 Fly ash

Class F fly ash was acquired from SMEET Qatar with chemical compositions specified in Table 1 complying with QCS 2014 and ASTM C618-12a standards [46]. Fly ash passing sieve #200 (75 µm) was used in the mix design for geopolymer mortar. Moisture content was conducted according to ASTM C 311 [47] and it was 0.5%. Fineness of fly ash is 11.3 %, which is measured by the percentage residue in 45 µm sieve. The fly ash density is 2.230 which was conducted according to ASTM C 188-16 [48].

Table 1. Chemical composition of Fly ash used in the study

Oxide	SiO_2	Al_2O_3	CaO	Fe_2O_3	MgO	SO_3	K_2O	Na_2O	Cl^-	LOI
%	49.9	17.1	11.8	7.83	4.9	0.42	0.2772	0.1428	0.011	3.5

3.1.2 Sand

Locally available silica sand with grade of 20-30 sand was used conforming to ASTM Standard C778 for mortar mixing [49]. The fineness modulus of the sand was 2.31, specific gravity of 2.56 and water absorption of 1.87%.

3.1.3 Activator solutions

3.1.3.1 Sodium hydroxide

Sodium hydroxide (NaOH) solution with concentrations of 12, 14 and 16 Molar were prepared by mixing 480, 560 and 640 gm of NaOH pellets in one liter of distilled water, respectively. Sodium hydroxide pellets with purity of 98 % was acquired from a local supplier with the composition depicted in Table 2.

Table 2. Checmical composition of NaOH pellets

Chemical composition	Percentage %
NaOH	98
Na2CO3	1
Cl	0.01
SO4	0.003
PO4	0.002
SIO2	0.01
N	0.0005
Heavy metals	0.0005
Fe	0.001
Al	0.001
As	0.0004
K	0.1

Sodium hydroxide pellets were dissolved gradually in distilled water until reaching the desired concentration of the solution. Each solution was prepared in big plastic container while the plastic container was in a water bath to accommodate the heat of the reaction between Sodium hydroxide and water as the reaction is exothermic reaction. The solution is left at room temperature for 30 mins to lower its temperature. The solution is poured in an airtight glass jar to prevent the reaction with air and to be used in the days to follow to prepare the different mix designs of geopolymer mortar as shown in Figure 6.

(a) (b) (c)

Figure 6. Sodium hydroxide; (a,b) pellets, (c) solution stored in a glass jar.

3.1.3.2 Sodium silicate

Sodium Silicate (Na_2SiO_3) solution was acquired from Qatar Detergent Company in Qatar with Sodium silicate (Na2SiO3) concentration of 40% to 60% water. The solution is prepared by mixing anhydrous sodium silicate crystals under heat and pressure with water. Figure 7 shows sodium silicate as crystals lumps and as a solution.

(a) (b)

Figure 7. Sodium silicate; (a) lumps, (b) solution

Both Sodium hydroxide and Sodium Silicate were prepared separately before casting the geopolymer specimens. Sodium hydroxide (NaOH) and Sodium Silicate (Na_2SiO_3) were mixed together prior to mixing it with source materials to produce GPM.

3.2 Test specimens and test matrix

In order to achieve the objectives of the research effectively. The test program is divided into three main phases. Each phase is designed to study the effect of certain number of parameters on the rheology and mechanical properties of geopolymer mortar.

3.2.1 Phase one

Phase one is designed to study the effect of Molarity of Sodium hydroxide solution, Fluid/binder ratio and Sodium silicate to Sodium hydroxide ratio. The fluid is the total amount of activators solution both of sodium silicate and hydroxide and the binder is the fly ash. Three different molarities were investigated in this study which are 12, 14 and 16 Molar the molarity factor is denoted by "M". Fluid to binder ratio were selected to be 0.60, 0.65 and 0.70 to be carried out in Phase one. These values were selected based on a preliminary study as it was found that any lower fluid to binder ratio leads to a mix design with very low workability. In the case where the fluid to binder ratio is higher than 0.70 the mix design had very high flowability. The effect of Sodium silicate to sodium hydroxide was investigated. Four ratios of 1, 1.5, 2 and 2.5 were selected based on the literature review. The molarity, fluid to binder ratio and sodium silicate to sodium hydroxide ratio were investigated together as they are internal factors directly affecting the mix design. Table 3 summarizes the factors included in phase 1 of this

study. The experimental matrix for phase 1 is summarized in Table 4. In phase one a total of 108 cubes were produced to find the optimum combination of the three factors. The best mix design from phase one was selected to continue the experimental study in phase 2.

Table 3. Summary of the parameters for phase 1

Molarity (M)	Fluid/ Binder F/B (F)	Na2siO3/NaoH (N)
12	0.60	1
14	0.65	1.5
16	0.70	2
N. A	N. A	2.5

Table 4. Experimental matrix for phase 1

#	Mix Design	N1	N2	N3	N4	Total
1	M1F1	3	3	3	3	12
2	M1F2	3	3	3	3	12
3	M1F3	3	3	3	3	12
4	M2F1	3	3	3	3	12
5	M2F2	3	3	3	3	12
6	M2F3	3	3	3	3	12
7	M3F1	3	3	3	3	12
8	M3F2	3	3	3	3	12
9	M3F3	3	3	3	3	12
						108

3.2.2 Phase two

is aimed to study the effect of curing duration and temperature on the mechanical properties of geopolymer mortar. In phase 2 a total of 27 geopolymer mortar cubes were casted. Three main curing duration were investigated in this study which are 24, 48 and 72 hrs. with three different curing temperatures of 40, 80 and 120 ^{0}C as shown in Table 5. The curing temperature is denoted by “T” and the curing duration is denoted by “D”. The experimental matrix for phase two is summarized in Table 6. In this phase the

external factors of curing duration and temperature are extremely important, as it will define best casting conditions for higher mechanical properties. The best curing conditions will be selected to continue the last phase of the study.

Table 5. Factors investigated in phase 2

Time (D) (hours)	Temperature (T) (^{o}C)
24	40
48	80
72	120

Table 6. Experimental program for Phase 2

Mix Design	T1	T2	T3	Total
D1	3	3	3	9
D2	3	3	3	9
D3	3	3	3	9
				27

3.2.3 Phase three

The effect of age on geopolymer mortar samples were investigated for two conditions. First condition is under heat curing where geopolymer mortar with best mix design and best curing conditions were tested. The second condition is to investigate the best mix design under curing of room temperature. Geopolymer samples at durations of 1, 3, 7 and 28 days were tested to investigate the strength gain over time. Table 7 shows the experimental test matrix for Phase 3.

Table 7. Experimental program for phase 3

#	Mix Design	0 Days	3 Days	7 Days	28 Days	Total
1	T,D,M,F,N	3	3	3	3	12
2	RT	3	3	3	3	12
						24

Three mortar cubes were casted in 5 cm cubes according to ASTM C109 standards [50]. The average of the three mortar cubes were reported for the compressive strength.

3.3 Mix designs

A total of 36 geopolymer mortar mix designs were prepared in this study. Fly ash to Sand ratio was fixed for all mix designs to 1:2.75. The details of the mix designs are depicted in Table 8. One mix design was activated using only Sodium hydroxide to examine the effect of the existence of sodium silicate solution. The naming of specimens is as shown in Figure 8 below.

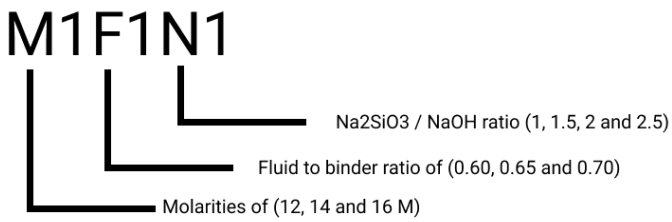

Figure 8. Nomenclature of GPM specimens

Table 8. Mix designs included in the study

Mix design ID	Fly ash (gm)	Sand (gm)	Alkaline activator/fly ash ratio	Na2sio3/NaOH ratio	NaOH solution (gm)	Na2SiO3 solution (gm)
F1N1	266.7	733.33	0.60	1	80.00	80.00
F1N2	266.7	733.33	0.60	1.5	64.00	96.00
F1N3	266.7	733.33	0.60	2	53.33	106.67
F1N4	266.7	733.33	0.60	2.5	45.71	114.29
F2N1	266.7	733.33	0.65	1	86.67	86.67
F2N2	266.7	733.33	0.65	1.5	69.33	104.00
F2N3	266.7	733.33	0.65	2	57.78	115.56
F2N4	266.7	733.33	0.65	2.5	49.52	123.81
F3N1	266.7	733.33	0.70	1	93.33	93.33
F3N2	266.7	733.33	0.70	1.5	74.67	112.00

Table 8. Mix designs included in the study

Mix design ID	Fly ash (gm)	Sand (gm)	Alkaline activator/fly ash ratio	Na2sio3/NaOH ratio	NaOH solution (gm)	Na2SiO3 solution (gm)
F3N3	266.7	733.33	0.70	2	62.22	124.44
F3N4	266.7	733.33	0.70	2.5	53.33	133.33
NaOH	266.7	733.33	0.60	-	160	-

3.3.1 Preparation of specimens

After weighing each material as specified in Table 8. The following steps were followed to produce geopolymer mortar.

1. Sodium Hydroxide and sodium silicate solutions were mixed together for 2 mins in a glass measuring jar.
2. The activator solutions were placed in the mixing bowl.
3. Fly ash was added to the activator solutions and mixed in the mixing bowl for 30 sec at low speed.
4. Sand was added to the mix and mixing continues for 30 sec at low speed.
5. The mixing speed increased to high speed and the mixing continues for 120 sec.
6. The flow table test is conducted, followed by 15 sec mixing at high speed.

The mortar then placed in 5 cm mortar cubes to be filled in two layers each layer is tamped by the tamping rod for 32 times according to ASTM C109 standards [51]. The excess of the mortar is removed by the trowel ensuring a flat surface. For phase 1 of the experimental program the molds were directly placed in the oven as the temperature and duration were fixed to 80 ^{0}C and left for curing for 24 hrs. The mixing procedures are summarized in Figure 9.

(a)

(b)

(c)

(d)

Figure 9. Mixing procedures; (a) Adding sand to the mix, (b) mixing of GPM, (c) Casting in cube molds, (d) oven curing of GPM.

3.3.2 Test setups

3.3.2.1 Compressive strength

The compressive strength of geopolymer mortar is conducted in a Controls universal testing machine according to ASTM standards as show in Figure 10. The loading rate was set to 1300 N/s with peak sensitivity of 5 kN. Geopolymer mortar samples were loaded till failure.

Figure 10. Universal compressive testing machine

3.3.2.2 Flow table test

The flow table was conducted for all mix designs prepared in this study. Geopolymer mortar were tamped 20 times by the tamper and any excess mortar were removed from surface then the table was dropped 25 times. Flow table test is reported by calculating the average of four readings minus the inside base diameter. The flow table test was conducted according to ASTM C1437 [52]. It is calculated by taking the average of four measurements of the diameter, minus the diameter of the inside base, divided by original inside base diameter as shown in Equation 1. of Figure 11 shows the setup for the flow table test.

$$flow\ (\%) = \frac{D.avg - D.inside}{D.inside} * 100$$

Figure 11. Setup for the flow table test

3.3.2.3 Scanning Electron Microscopy (SEM)

Scanning Electron Microscopy was conducted on seven geopolymer mortar samples. The SEM analysis was conducted in the Central lab unit at Qatar university on NOVA NanoSEM 450 device as shown in Figure 12. To study the variations of the internal structure of geopolymer mortar due to the different factors investigated in this study. The effect of using different molarities of the activator solution on the internal structure of GPM activated using sodium hydroxide with molarities of 12,14 and 16 M and sodium silicate were investigated. Geopolymer mortar activated with sodium hydroxide only with molarity of 12 M was investigated to examine the effect of sodium

silicate solution on the development of the polymerization products. The effect of different curing temperatures on the internal structure of GPM were examined. Magnifications of 2500 and 5000 x were performed on all specimens for comparison.

Figure 12. Scanning electron microscopy device

The procedure of conducting SEM analysis was per ASTM C1723 standards [53]. Fractured pieces of a size of 0.5 cm of geopolymer mortar were placed on a metallic round holder for analysis as shown in Figure 13a. As geopolymer mortar are poor conductors, gold coating was applied on the specimens for 40 sec as specified in ASTM C1723 standard as shown in Figure 13b.

(a) (b)

Figure 13. SEM sample preparation; (a) Metal holder, (b) Applying gold coat to improve conductivity.

3.3.2.4 X-Ray Diffraction analysis (XRD)

X-Ray Diffraction analysis was performed on the grinded samples of geopolymer mortar. The samples were grinded using a ball milling machine as shown in Figure 14. After conducting the compressive strength test the mortar were preserved in airtight plastic bags to prevent any contamination of the GPM with any foreign materials. The samples were grinded for 10 mins at a speed of 300 rpm. The samples were placed on XRD machine to obtain the crystallographic characterization of the constituents of the materials. The output of the XRD analysis are the peaks where the constituent elements can be identified, thus XRD analysis is a qualitative analysis and was conducted according to ASTM C1365 [54] .

(a) (b)

Figure 14. Grinding samples; (a) GPM fractured specimens, (b) powdering of specimens.

3.3.2.5 Energy dispersive X-ray spectroscopy (EDS)

EDS analysis was performed to quantify the elements available in different mixes of GPM. The EDS was conducted according to ASTM E1508 [55]. The EDS was conducted using NOVA NanoSEM 450 device. EDS analysis gives a quantitative analysis of SEM samples.

CHAPTER 4: RESULTS AND DISCUSSIONS

4.1 Compressive strength

The variations in compressive strength due to molarity, fluid to binder ratio, sodium silicate to sodium hydroxide ratio, effect of curing conditions and age of geopolymer mortar were reported and discussed in the subsections below. The results were compared and correlated with the literature.

4.1.1 Effect of Molarity

As mentioned in chapter 3, three molarities of 12, 14 and 16M were investigated in this study. The curing conditions were fixed at 80 ^{0}C and curing duration of 24 hrs. In order to explain the effect of using different molarities of sodium hydroxide (NaOH) solution, for each fluid to binder ratio and sodium silicate to sodium hydroxide ratio a comparison was conducted.

For fluid to binder ratio of 0.60 it was noted that sodium hydroxide solution with molarity of 16 M exhibited the highest compressive strength of more than 60 MPa for all sodium silicate to sodium hydroxide ratios of 1, 1.5, 2 and 2.5. An increasing trend of the compressive strength was noted across the molarities of sodium hydroxide solution, as the molarity increases the compressive strength increase for different sodium silicate to sodium hydroxide ratio as shown in Figure 15. Further, the minimum compressive strength of geopolymer mortar activated by sodium hydroxide solution of 12 M was attained by mix design of F1N1 of 33.4 MPa.

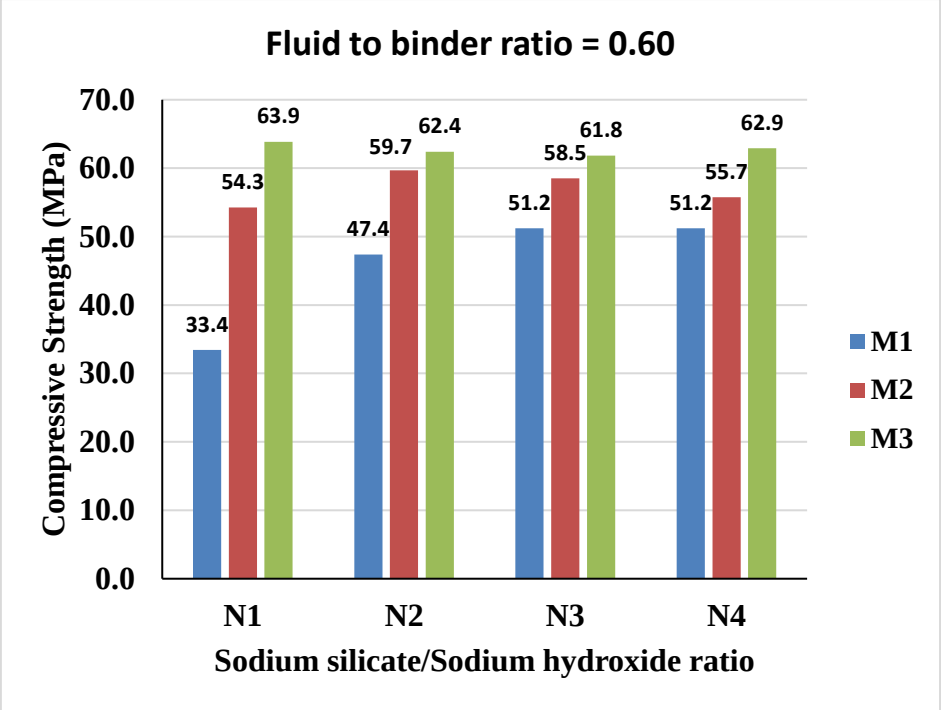

Figure 15. Effect of molarity at F/B ratio of 0.60

For fluid to binder ratio of 0.65 it was noted that the maximum compressive strength was attained by mix design activated by sodium hydroxide of 14 M and with sodium silicate to sodium hydroxide ratio of 2 and it was 61.6 MPa. The minimum compressive strength was equal to 45.1 MPa attained by mix design activated by sodium hydroxide of 14 M and with sodium silicate to sodium hydroxide ratio of 1 as shown in Figure 16. Further, it can be observed that the compressive strength for GPM mix designs with 0.65 fluid to binder ratio and with sodium silicate to sodium hydroxide ratio of 1 and 1.5 had little variations in the compressive strength. On the other hand, GPM mix designs with sodium silicate to sodium hydroxide ratio of 2.5 showed a similar increasing trend for the compressive strength as the molarity increased.

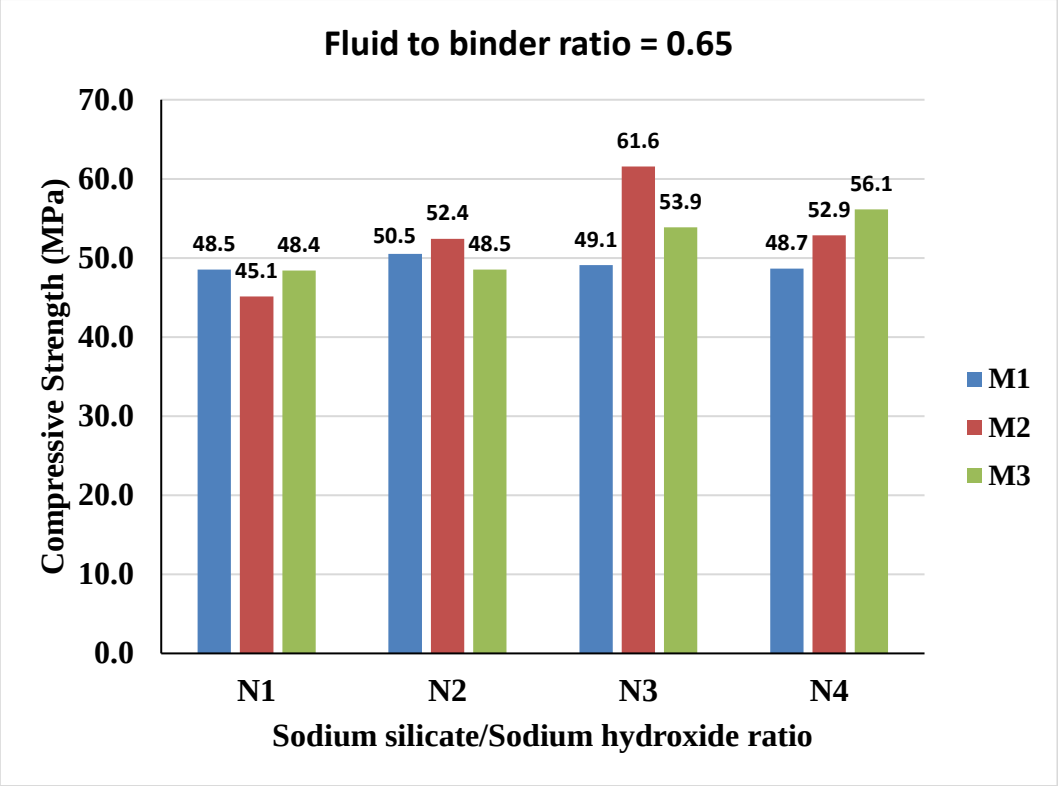

Figure 16. Effect of molarity at F/B ratio of 0.65

For fluid to binder ratio of 0.70 the effect of molarity to the compressive strength varied across different sodium silicate to sodium hydroxide ratio as shown in Figure 17. For a Na2SiO3/NaOH ratio of 1, the compressive strength was the highest for GPM activated with 12M NaOH solution. However, the trend for the compressive strength for GPM activated with 12M NaOH decreases as the Na2SiO3/NaOH increased. For specimens activated with 14M NaOH alkaline solution, it was noted that the compressive strength increased as the Na2SiO3/NaOH increased till a ratio of 2, for the Na2SiO3/NaOH ratio of 2.5 the compressive strength slightly decreased. For GPM activated with 16M NaOH solution the compressive strength decreased along the Na2SiO3/NaOH ratios of 1,1.5 and 2. However, the compressive strength increased for Na2SiO3/NaOH ratio of 2.5. The maximum compressive strength of 53 MPa was attained by 14M NaOH alkaline solution with Na2SiO3/NaOH ratio of 2, and the minimum compressive strength of

36.8 MPa was attained by GPM activated with 16M NaOH alkaline solution with Na2SiO3/NaOH ratio of 2.

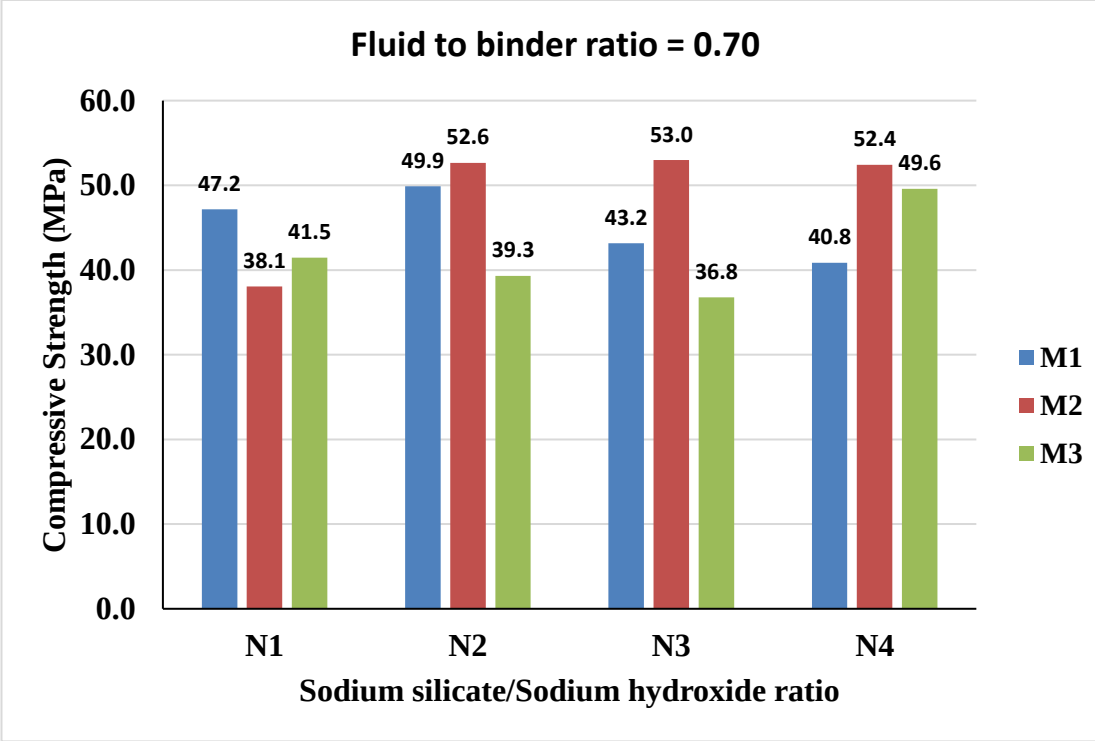

Figure 17.Effect of molarity at F/B ratio of 0.70

The effect of molarity on the compressive strength of GPM was investigated by multiple authors, who concluded that the compressive strength increases as the molarity of NaOH solution increases [40], [56], [57]. Görhan & Kürklü (2014) studied three different concentrations of NaOH solution of 3, 6 and 9M. The results showed that highest compressive strength was attained by GPM mix activated by 9M NaOH solution. However, there are limited studies that investigated the combined effect of fluid to binder ratio with sodium silicate to sodium hydroxide ratio at different molarities.

4.1.2 Effect of Fluid to binder ratio

The effect of fluid to binder ratio was investigated with three different ratios of (0.60, 0.65 and 0.70) as mentioned in chapter 3. Each molarity of the NaOH solution was fixed and investigated along different ratios of Na2SiO3/NaOH. Three graphs were generated to study and compare the effect of fluid to binder ratio on the compressive strength of GPM for different molarities of NaOH solutions.

The effect of fluid to binder ratio was investigated for GPM mix designs activated with 12 M NaOH alkaline solution as shown in Figure 18. It was noted that for Na2SiO3/NaOH ratio of 1 and 1.5, the compressive strength for fluid to binder ratio of 0.60 was lower than this of both GPM with fluid to binder ratios of 0.65 and 0.70. However, for fluid to binder ratio of 0.6 and Na2SiO3/NaOH ratios of 2 and 2.5, the compressive strength was the highest reaching 51.2 MPa. Further, it can be noted that for Na2SiO3/NaOH ratios of 2 and 2.5 there is a decreasing trend of the compressive strength as the fluid to binder ratio increases from 0.60 to 0.70. The minimum compressive strength was attained by GPM mix design of M1F1N1 of 33.4 MPa, and the maximum compressive strength was attained by two mix design of M1F1N3 and M1F1N4 reaching 51.2 MPa.

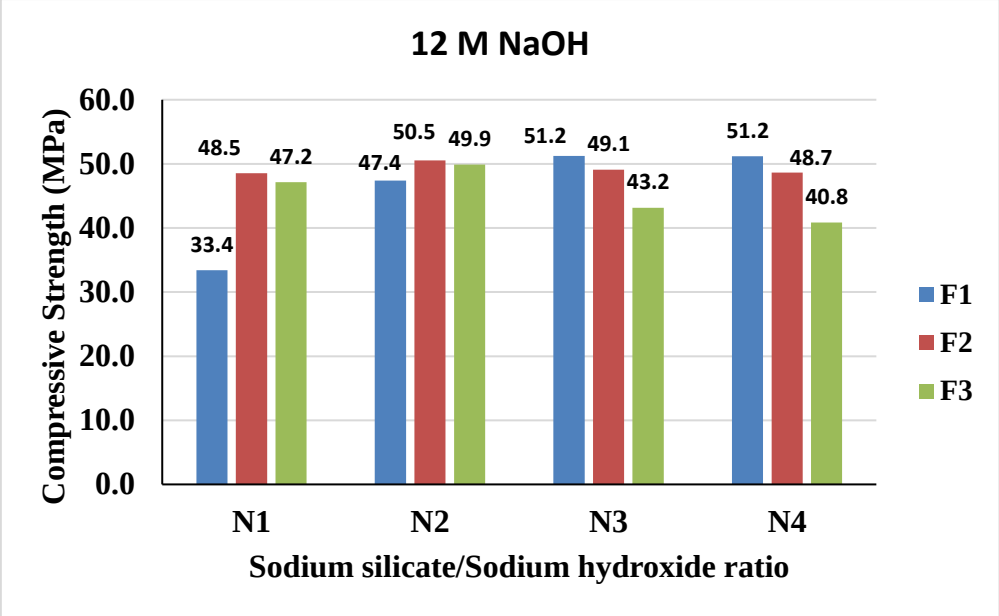

Figure 18. Effect of F/B ratio at 12 M NaOH solution

The effect of fluid to binder ratio for GPM activated with 14 M NaOH solution is shown in Figure 19. It was noted that the compressive strength decreased as the fluid to binder ratio increase for Na2SiO3/NaOH ratio of 1 and 2.5. For GPM mix designs with Na2SiO3/NaOH ratio of 1.5 the maximum compressive strength of 59.7 MPa was attained by samples with fluid to binder ratio of 0.60, there were little differences in the compressive strength for fluid to binder ratios of 0.65 and 0.70. The maximum compressive strength was attained by GPM mix design of M2F2N3 of 61.6 MPa, and the minimum compressive strength of 38.1 MPa was attained by GPM mix design of M2F3N1.

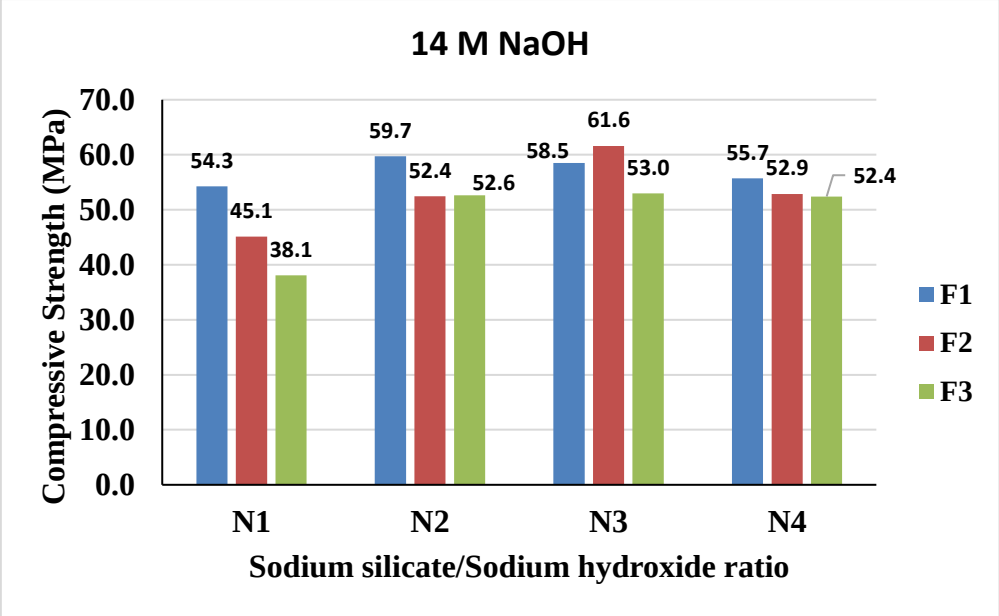

Figure 19.Effect of F/B ratio at 14 M NaOH solution

The effect of fluid to binder ratio for GPM specimens activated by NaOH solution with a concentration of 16M was investigated as shown in Figure 20. The results showed that GPM specimens with fluid to binder ratio of 0.60 exhibited the maximum compressive strength for all Na2SiO3/NaOH ratios. As it can be noted that there is a decreasing trend in the compressive strength for GPM specimens across all Na2SiO3/NaOH ratios. The maximum compressive strength of 63.9 MPa was attained by GPM mix design of M3F1N1. Further it can be noted that GPM specimens attained with fluid to binder ratio of 0.65 attained the second highest compressive strength for all Na2SiO3/NaOH ratios, and the lowest compressive strength of GPM specimens were attained by mixes with fluid to binder ratio of 0.70. A minimum compressive strength of 36.8 MPa was attained by GPM design of M3F3N2.

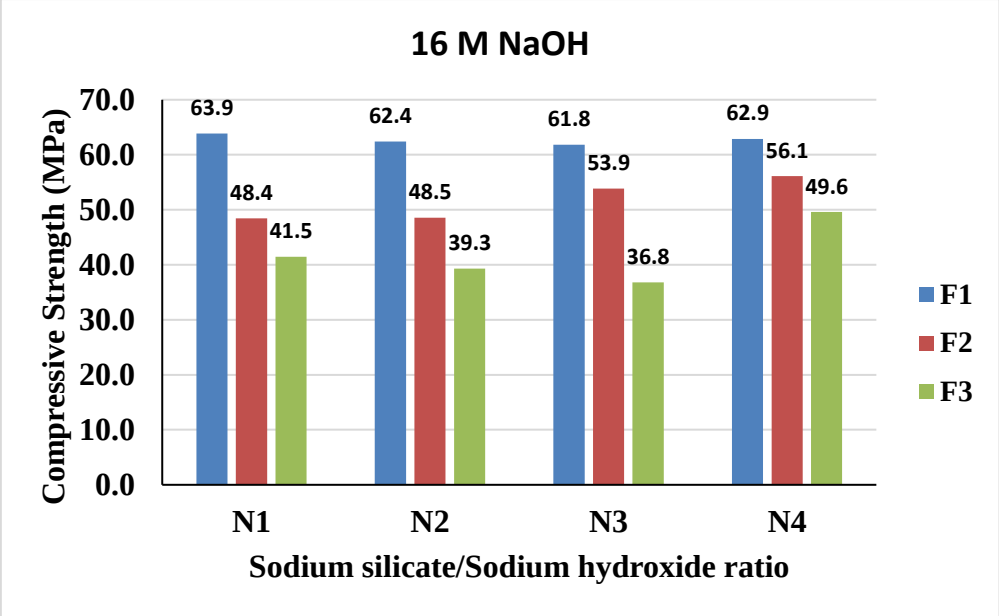

Figure 20. Effect of F/B ratio at 16 M NaOH solution

The effect of fluid to binder ratio on the compressive strength of GPM varied for different molarities. For GPM specimens activated with 16M NaOH solution, the decreasing trend in the compressive strength was clear, which means that as fluid to binder ratio increases the compressive strength decreases. This might be attributed to the excess amount of hydroxide ions in the mix, similar findings were reported by [58]–[60].

4.1.3 Effect of Na2SiO3/NaOH

The effect of sodium silicate to sodium hydroxide ratio was investigated. Four different ratios of 1, 1.5, 2 and 2.5 were examined. In order to visualize the effect of Na2SiO3/NaOH ratios on the compressive strength of GPM, each molarity was studied separately for different fluid to binder ratios.

For GPM mix designs activated with 12M NaOH solution the compressive for different Na2SiO3/NaOH ratios is shown in Figure 21. It can be noted that for fluid to binder ratio of 0.60 and Na2SiO3/NaOH ratio of 1 a minimum compressive strength of 33.4

MPa was achieved. However, the increase in Na2SiO3/NaOH ratio to 1.5 increased the compressive strength to reach 47.4 MPa. Further, it can be noted that the compressive strength did not change for Na2SiO3/NaOH ratio of 2 and 2.5 reaching 51.2 MPa. For fluid to binder ratio of 1.5 the difference in the compressive strength between GPM mixes with different Na2SiO3/NaOH ratios were insignificant, with a maximum compressive strength reaching 50.5 MPa. Further, it can be noted that the compressive strength did not change for Na2SiO3/NaOH ratio of 2 and 2.5 reaching 49.1 MPa. For fluid to binder ratio of 0.70 a maximum compressive strength of 49.9 MPa was achieved by mix design of M1F3N2. Further, it can be noted that the compressive strength did not change for Na2SiO3/NaOH ratio of 2 and 2.5 reaching 43.2 MPa.

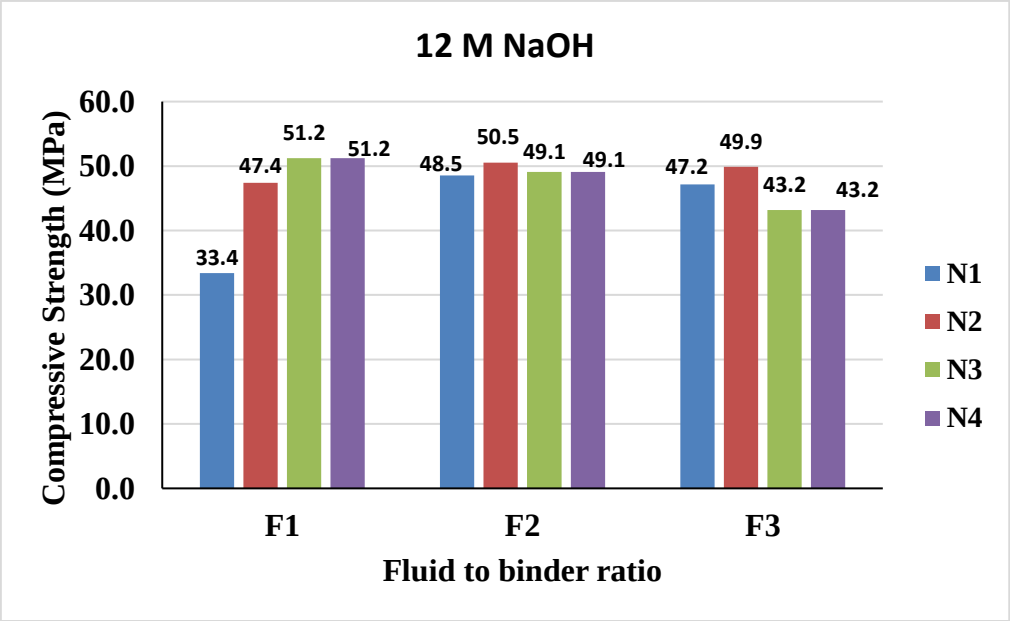

Figure 21. Effect of Na2Sio3/NaOH ratio at 12 M NaOH solution

For GPM mix designs activated with 14M NaOH solution the compressive strength was varying for different fluid to binder ratios as shown in Figure 22. For fluid to binder ratio of 0.60 a maximum compressive strength of 59.7 MPa was achieved by GPM mix of M2F2N2 and minimum compressive strength of 54.3 MPa. Moreover, it was noted

that for fluid to binder ratio of 0.60 and Na2SiO3/NaOH ratios of 1.5, 2 and 2.5 there was a decreasing trend in the compressive strength as the Na2SiO3/NaOH ratio increased.

For fluid to binder ratio of 0.65, the effect of Na2SiO3/NaOH ratio on the compressive strength of GPM specimens increased as increasing Na2SiO3/NaOH ratios of 1, 1.5 and 2, reaching a maximum of 61.6 MPa, however for Na2SiO3/NaOH ratio of 2.5 the compressive strength decreased to reach 52.9 MPa.

For GPM specimens with fluid to binder ratio of 0.70 and Na2SiO3/NaOH ratio of 1 the compressive strength was the lowest reaching 38.1 MPa. However, for Na2SiO3/NaOH ratios of 1.5, 2 and 2.5 the compressive strength were almost the same for all GPM specimens reaching a maximum value of 53.0 MPa.

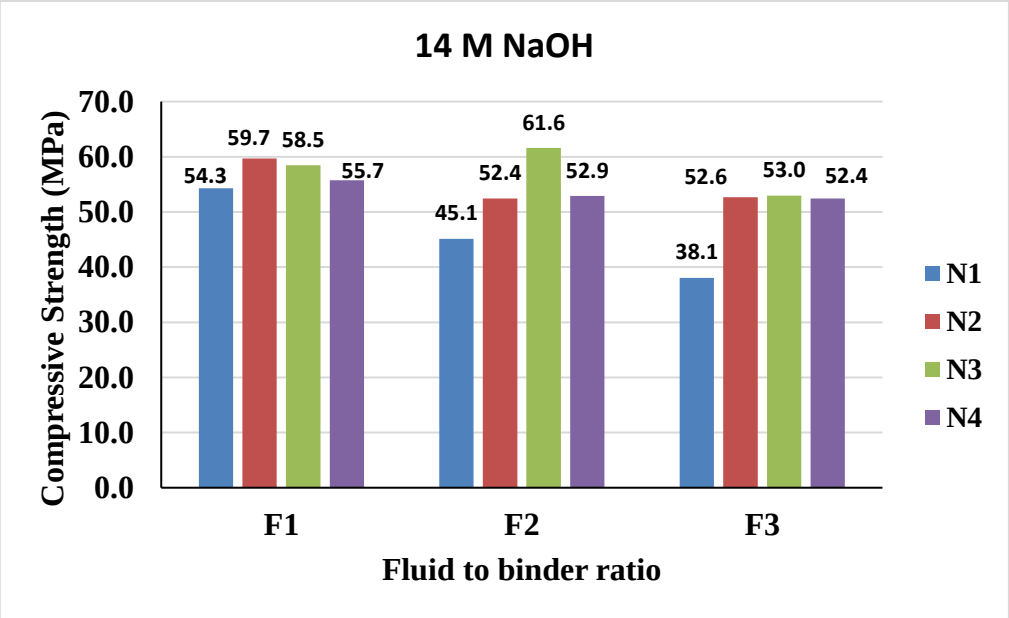

Figure 22.Effect of Na2Sio3/NaOH ratio at 14 M NaOH solution

For GPM mix designs activated with 16M NaOH solution the compressive strength was the highest for fluid to binder ratio of 0.60 with Na2SiO3/NaOH ratios of 1, 1.5, 2 and 2.5 reaching a maximum value of 63.9 MPa as shown in Figure 23. For fluid to binder ratio of 0.65 the compressive strength decreased compared to GPM mixes with fluid to

binder ratio of 0.60, reaching a maximum of 56.1 MPa and a minimum of 48.4 MPa. For fluid to binder ratio of 0.70 the compressive strength was decreasing for Na2SiO3/NaOH ratios of 1, 1.5 and 2 starting from 41.5 MPa reaching 36.8 MPa, and for Na2SiO3/NaOH ratio of 2.5 it increased to reach 49.6 MPa. The minimum compressive strength was 36. 8 MPa attained by GPM mix design of M3F3N3.

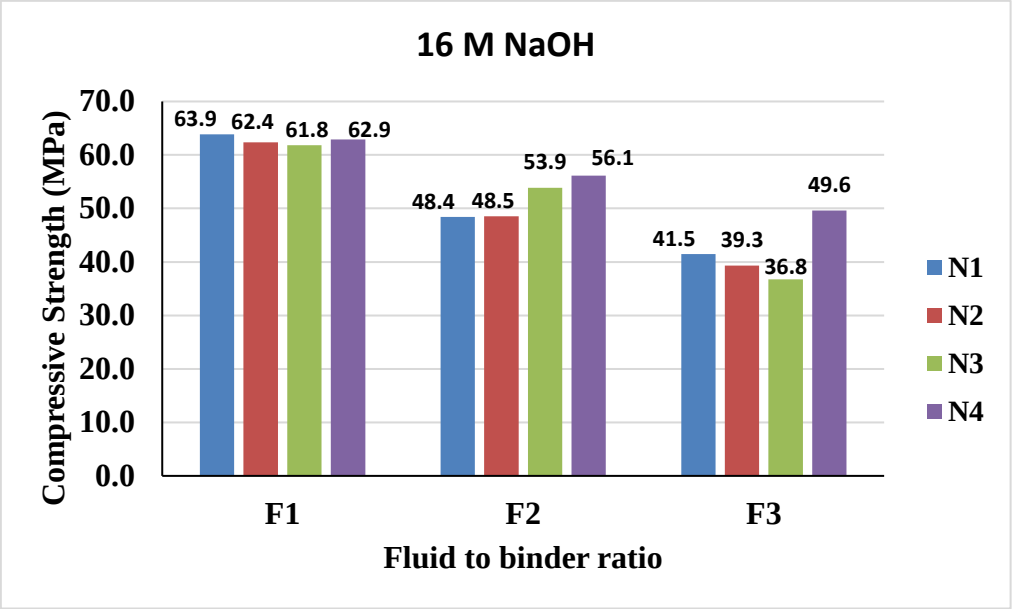

Figure 23.Effect of Na2Sio3/NaOH ratio at 16 M NaOH solution

4.1.4 Curing conditions

4.1.4.1 Effect of curing temperature

Curing temperature is considered one of the critical factors that affects the mechanical properties of GPM, as the presence of heat temperature accelerates the formation of the polymerization products. In order to study the effect curing temperature on the mechanical properties of GPM, mix design M3F1N1 was used to conduct the experimental work, as it attained the highest compressive strength of all mix design conducted in Phase one of the experimental program. Three temperatures of 40, 80 and 120 ^{o}C were studied as mentioned in chapter 3. Further, three durations

of 24, 48 and 72 hrs. were examined as shown in Figure 24.

The compressive strength for GPM specimens was following a specific pattern as there was a change in the curing temperature. The compressive strength increases by increasing the temperature until it reaches 80 ^{o}C then it decreases at curing temperature of 120 ^{o}C. For GPM specimens cured for 24 hrs. the highest compressive strength of 43.13 MPa was for samples cured at 80 ^{o}C, and minimum compressive strength of 19.83 MPa. For GPM specimens cured for 48 hrs. the highest compressive strength of 39.80 MPa was for samples cured at 80 ^{o}C, and minimum compressive strength of 18.17 MPa. For GPM specimens cured for 72 hrs. the highest compressive strength of 29.98 MPa was for samples cured at 80 ^{o}C, and minimum compressive strength of 24.37 MPa.

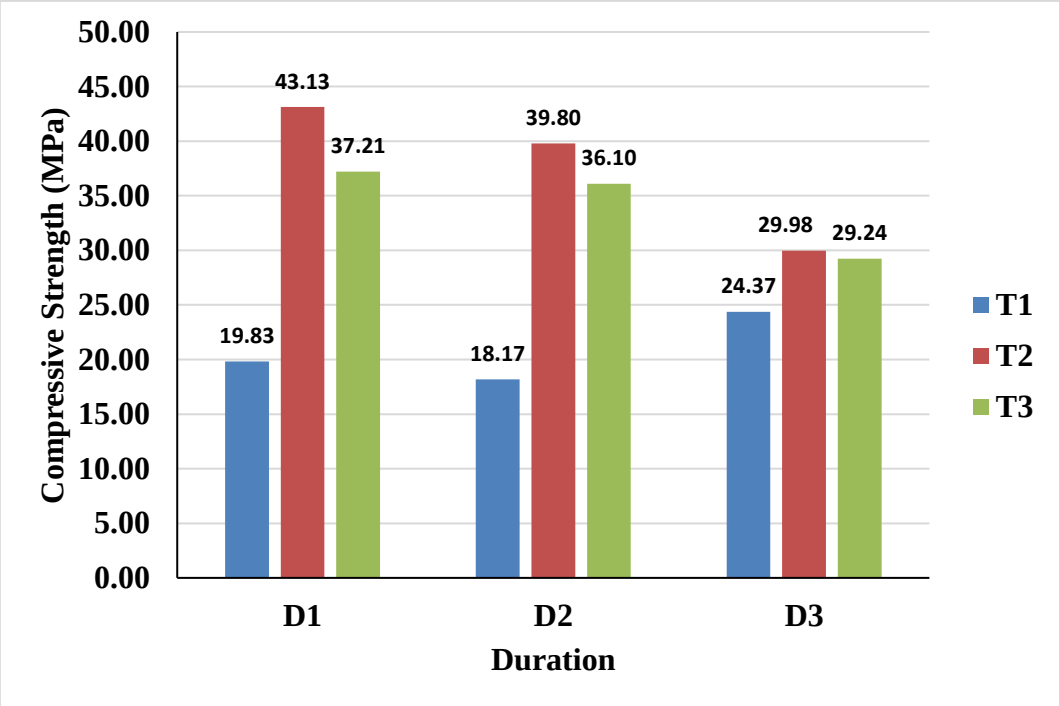

Figure 24. Effect of temperatures along different durations

Similar results were reported by multiple authors on the importance of heat curing in the development of compressive strength for geopolymers [32], [41], [45], [61].

It can be highlighted that the reason behind the increase in the compressive strength as the curing temperature increases till it reaches to 80 ^{o}C, and decreases when the temperatures goes to 120 ^{o}C can be attributed to the escape of water that exist in the activator solutions leaving behind numerous voids that affects the integrity of the matrix [62].

4.1.4.2 Effect of curing duration

The curing duration along with heat curing are two of the factors that directly influence the mechanical properties of GPM. In order to illustrate the effect of the curing duration on the compressive strength of GPM, each temperature was investigated and separately as shown in Figure 24.

It can be noted that for GPM cured at 40 ^{o}C exhibited the lowest compressive strength compared to all other curing temperatures investigated. Moreover, for GPM samples cured at 40 ^{o}C there was a decreasing trend in the compressive strength for durations of 24 and 48 hrs., then it increased to reach 24.4 MPa for curing duration of 72 hrs.

For GPM specimens cured at 80 ^{o}C attained the highest compressive strength among all curing temperature and for all curing durations. A maximum compressive strength of 43.1 MPa was achieved for samples cured for 24 hrs. It can be noted from Figure 24 the decreasing trend in the compressive strength as the curing duration increased reaching to 30 MPa for curing duration of 72 hrs.

For GPM specimens cured at 120 ^{o}C exhibited a compressive strength higher than GPM samples cured at 40 ^{o}C and lower compressive strength than GPM samples cured at 80 ^{o}C. It can be further noted that the decreasing trend in the compressive strength as the curing duration increased, similar trend was found by GPM samples cured at 80 ^{o}C.

The loss of strength as the duration increase might be attributed to the breakup of the amorphous structure of geopolymer mortar exposing the matrix to extensive moisture loss [63].

The experimental work conducted for heat curing shows that the best curing conditions for the mechanical properties of geopolymer mortar are a heat curing temperature of 80 ^{o}C and for a duration of 24 hrs.

4.1.5 Effect of age

The strength development over time is one of the properties that determines the maximum compressive strength the material can reach over time. Two different curing conditions were examined. The first condition is the heat curing condition, where GPM specimens were heat curing temperature of 80 ^{o}C and for a duration of 24 hrs. The second condition was GPM specimens cured at RT of 25 ^{o}C. Figure 25 shows the compressive strength for both heat and RT cured samples. It can be noted that the early development of the compressive strength for heat cured GPM specimens for the 0 days as it attained 43.1 MPa compared to GPM specimens cured at room temperature reaching 3.9 MPa. At three days of age heat cured GPM specimens did not gain any compressive strength reaching 42.1 MPa. However, for room temperature cured specimens there was a slight gain in the compressive strength by 3.4 MPa, similar findings were reported by [64]. At seven days the compressive strength for both RT and heat cured GPM specimens increased to 12.2, 51.1 MPa, respectively. At 28 days the compressive strength of heat cured GPM specimens reached 55 MPa, while the compressive strength for RT cured GPM specimens reached 20 MPa. It can be noted that the age affected both heat and RT cured specimens. For heat cured GPM specimen’s high early development of the compressive strength was achieved, at 28

days 30 % of the strength was gained due to the age. For RT specimens the strength development over 28 days period was noticeable as it increased by 4 times the compressive strength at 0 days, might be attributed to availability of moisture from the activator solution that is slowly reacting with the unreacted fly ash particles [65], [66]. These results emphasize on the importance of heat curing to achieve high mechanical properties.

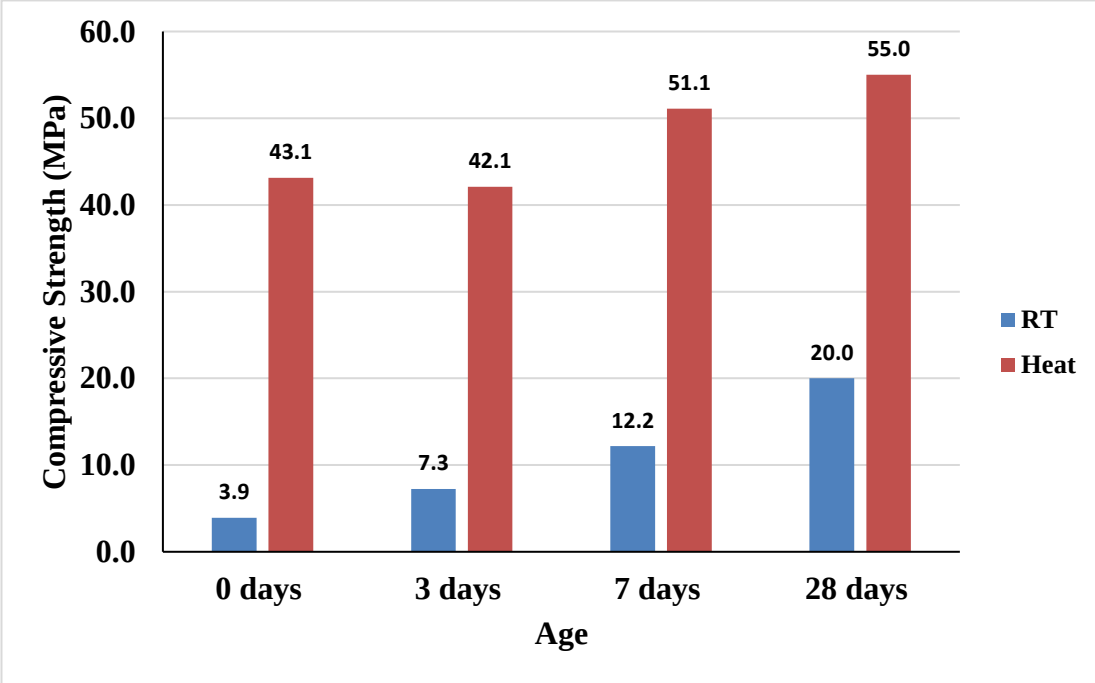

Figure 25. Effect of age on the strength development of GPM

4.1.6 Failure modes

The failure mode observed from testing GPM specimens under compression was similar in all mix designs. During the compression tests, GPM failed explosively, which indicates brittle failure. The cracks occurred at 45 degrees for all specimens with fragment separation out of specimens as shown in Figure 26. It was observed that the color of GPM samples cured at different temperatures varied, as it appeared to be darker

in color for specimens cured at lower temperature and it becomes more brighter as the temperature increases, this can be attributed to the degree where there are still moist/solution in the GPM samples as shown in Figure 27.

(a) (b)

Figure 26. Failure mode for most of GPM specimens at 45 degrees

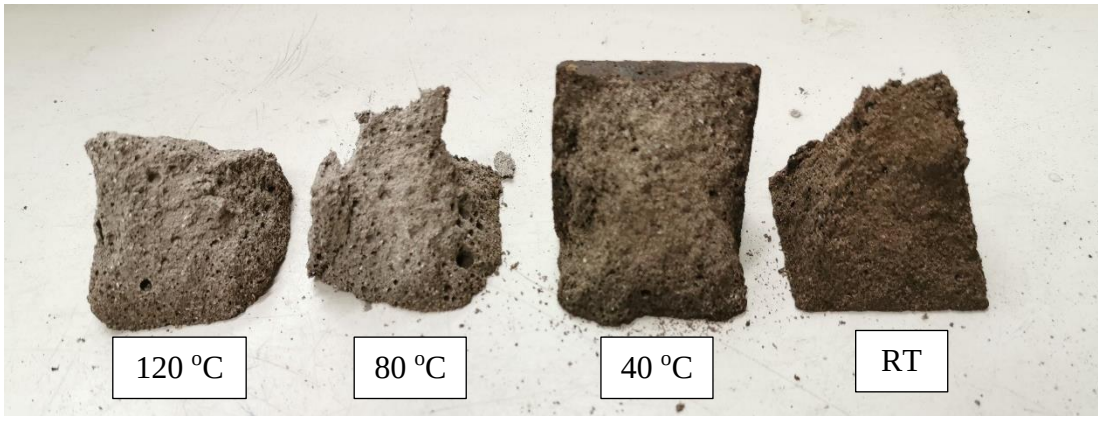

Figure 27. Visual appearance of GPM cured at different temperatures

4.2 Flow table test

The Flow table test was conducted for all GPM mix design specimens according to ASTM C230 [67] as mentioned in Chapter 3. The flow of GPM is reported in both the average diameter and the percentage of the flow relative to the inside base of the conical mold of the testing apparatus. The significance of this test is to check the workability of the GPM, which directly impact the quality, appearance and it determines how easy GPM can be placed and finished without having any concerns regarding the consistency. Table 9 below shows the results of the flow table test for all geopolymer mortar mix designs.

Table 9. Summary of flow table test

Mix design	Davg (cm)	Flow (%)
M1F1N1	14.81	48.13
M1F1N2	17.81	78.13
M1F1N3	20.38	103.75
M1F1N4	20.00	100.00
M1F2N1	20.13	101.25
M1F2N2	20.81	108.13
M1F2N3	20.81	108.13
M1F2N4	21.00	110.00
M1F3N1	22.56	125.63
M1F3N2	21.06	110.63
M1F3N3	21.81	118.13
M1F3N4	23.06	130.63
M2F1N1	15.50	55.00
M2F1N2	16.69	66.88
M2F1N3	18.00	80.00
M2F1N4	20.06	100.63
M2F2N1	20.00	100.00
M2F2N2	18.38	83.75
M2F2N3	19.06	90.63
M2F2N4	21.13	111.25
M2F3N1	23.19	131.88
M2F3N2	22.19	121.88
M2F3N3	19.42	94.17
M2F3N4	21.44	114.38

Table 9. Summary of flow table test

Mix design	Davg (cm)	Flow (%)
M3F1N1	19.31	93.13
M3F1N2	16.56	65.63
M3F1N3	16.19	61.88
M3F1N4	18.50	85.00
M3F2N1	19.69	96.88
M3F2N2	16.13	61.25
M3F2N3	15.13	51.25
M3F2N4	18.63	86.25
M3F3N1	19.31	93.13
M3F3N2	20.13	101.25
M3F3N3	17.31	73.13
M3F3N4	20.94	109.38

It can be noted from Table 9, that there were GPM mixes with high flowability and others with low flowability. Minimum flowability was attained by mix design M1F1N1 of 48.13% as shown in Figure 28.

Figure 28. Flow table test for GPM mix design M1F1N1

The maximum flowability of GPM was attained by GPM mix design of M2F3N1 of 131.8 % as shown in Figure 29.

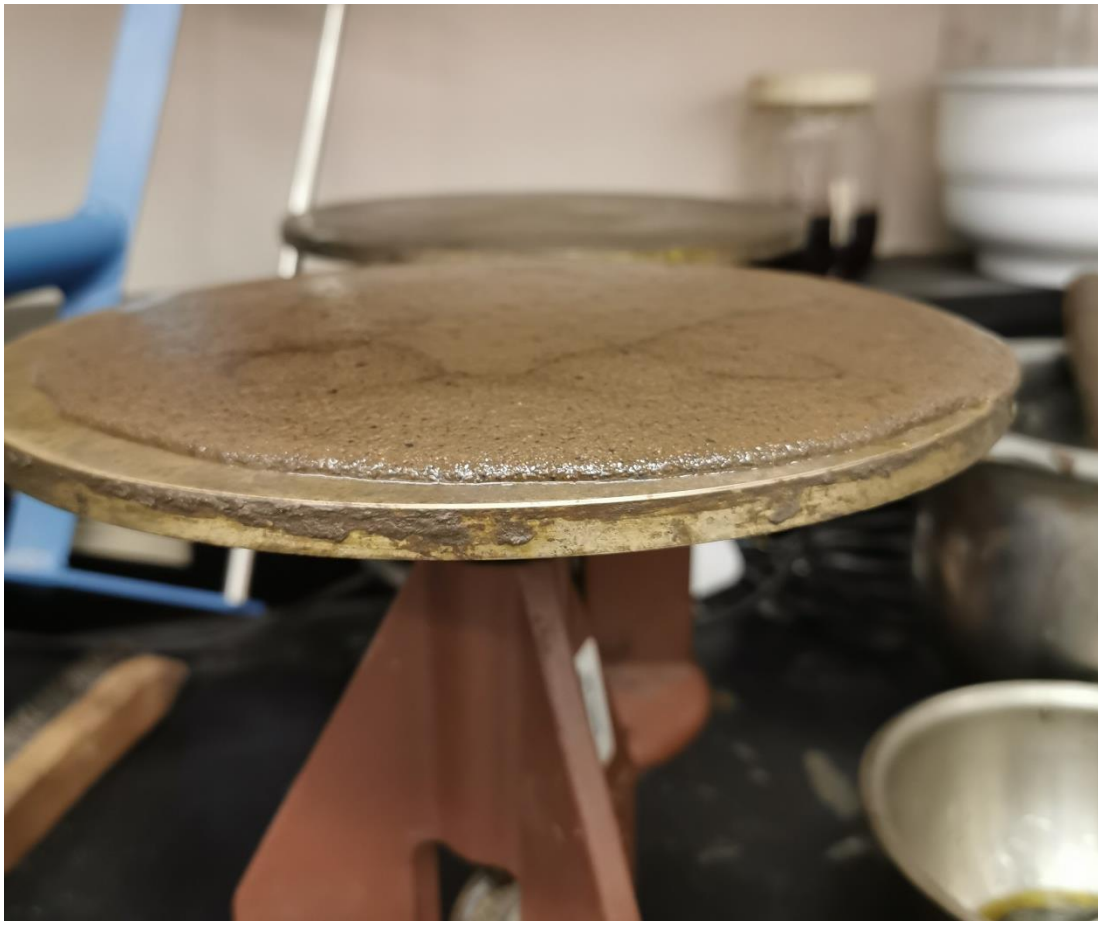

Figure 29. Flow table test for GPM mix design M2F3N1

It was observed for the same molarity the flowability of GPM increases as the ratio of Na2SiO3/NaOH increases. Further, it was noted during mixing the activators solutions of NaOH and Na2SiO3 together, prior mixing it with the source materials, the gelation process starts and the viscosity of the resultant solution increases, which reduces the flowability of GPM specimens. Based on the experimental work a recommended time limit of 5 mins of mixing the solutions together prior to continuing the procedures for mixing. Further, it was noted that during mixing the activators solutions of NaOH and Na2SiO3 together the temperature of the mixed solutions increases, which might affect the flowability of the mixed solution. Therefore, all mixed solution was left for a maximum of 5 mins to let the temperature drop to room temperature. It can be noted

that as the fluid to binder ratio increases the flowability of GPM mix increases as well, this can be attributed to the increase in the total amount of the solution available in the mix [68]–[70].

4.3 Microstructural Analysis

The microstructural analysis was done for seven GPM specimens to visually investigate the development of the geopolymerization products for different GPM mixes. In order to study the effect of molarity of sodium hydroxide solution three mix designs were examined, namely M1F1N1, M2F1N1 and M3F1N1. Moreover, the effect of curing temperature on GPM specimens was investigated through SEM, GPM specimens at temperatures of 40, 80 and 120 ^{o}C and cured for a duration of 48 hrs. Further, one GPM specimen activated using sodium hydroxide solution only was investigated, to study how the presence of sodium silicate affects the development of the geopolymerization products. Magnifications of 2500 X and 5000 X were used to visually inspect GPM specimens.

4.3.1 Effect of molarity

The effect of molarity of sodium hydroxide solution was studied using SEM for GPM mix designs of M1F1N1, M2F1N1 and M3F1N1 with compressive strengths of 33.4 54.3 and 63.9 MPa, respectively. Figure 30 shows the SEM images for GPM mix design of M1F1N1. It can be noted that the existence of pores in the matrix with reacted and unreacted FA particles, with the amorphous geopolymerization products. GPM contains mainly structures of the types Q_4 (2Al) and Q_4 (3Al). As found by Alehyen et al. (2017) The microstructure of geopolymer specimens reveals the formation of heterogeneous matrix which consists of a dense continuous gel-like with microcracks

and micropores [71].

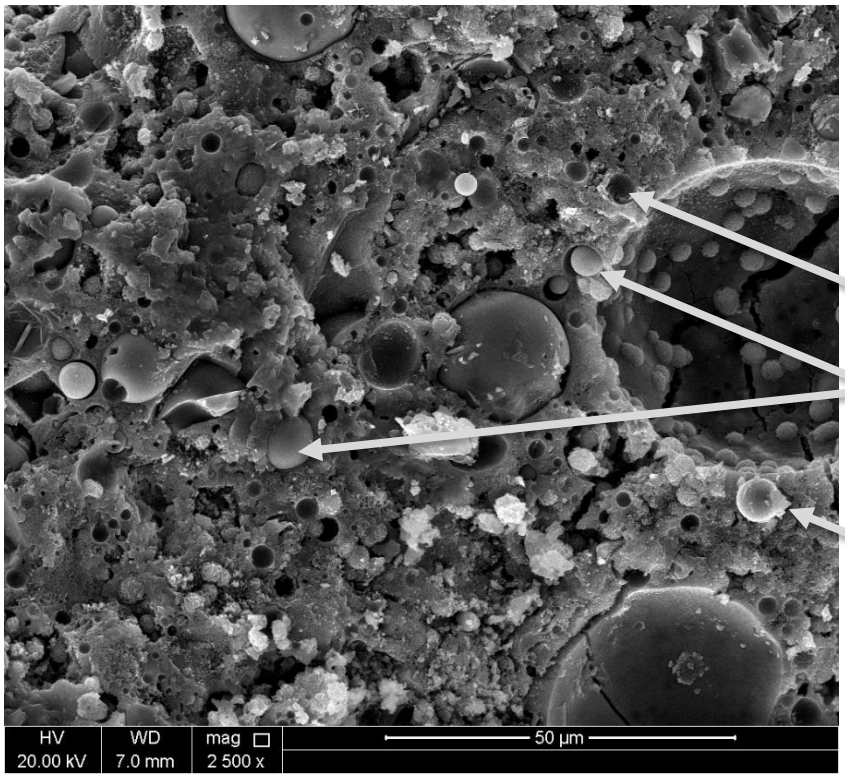

M1F1N1

fc = 33.4 MPa

2500x Mag.

Voids

Unreacted FA

Reacted FA

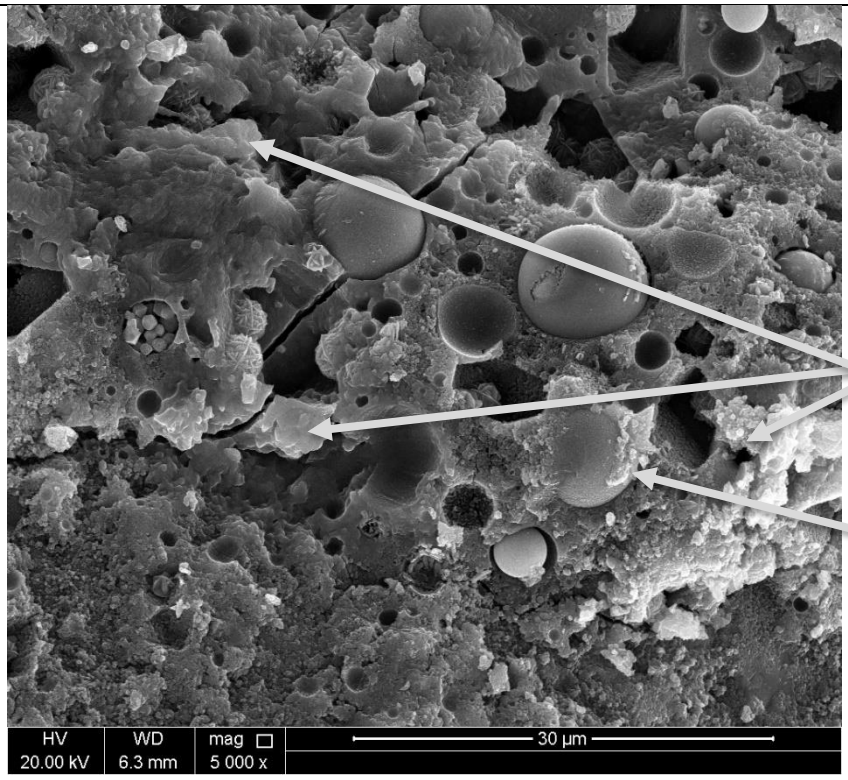

M1F1N1

fc = 33.4 MPa

5000x Mag.

Geopolymer

matrix

Reacted FA

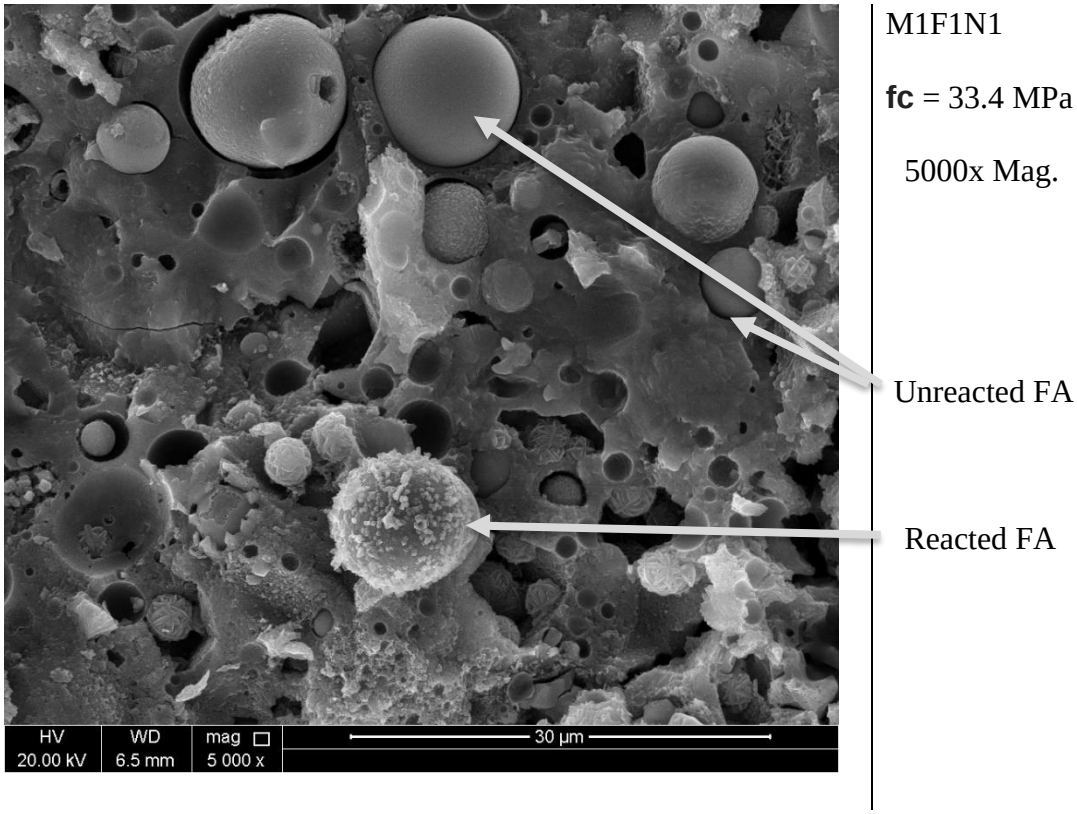

Figure 30. SEM Images for GPM mix design M1F1N1

Figure 31 shows the SEM images for mix design M2F1N1 that attained a compressive strength of 54.3 MPa. It can be noted the polymerization matrix is denser than M1F1N1 and there are more reacted FA particles with less pores in the matrix.

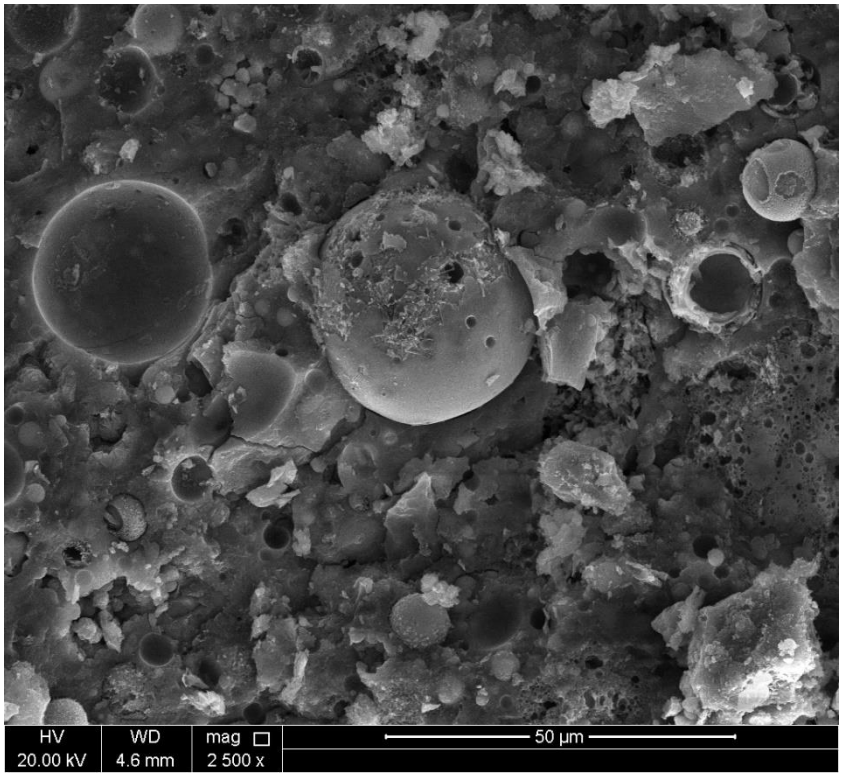

M2F1N1

fc = 54.3 MPa

2500x Mag.

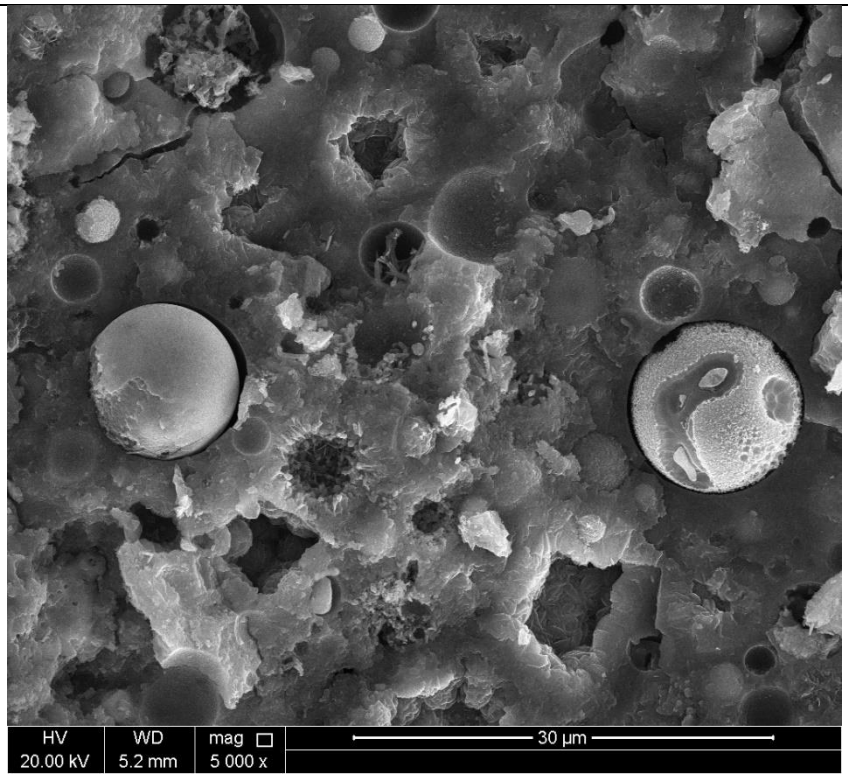

M2F1N1

fc = 54.3 MPa

5000x Mag.

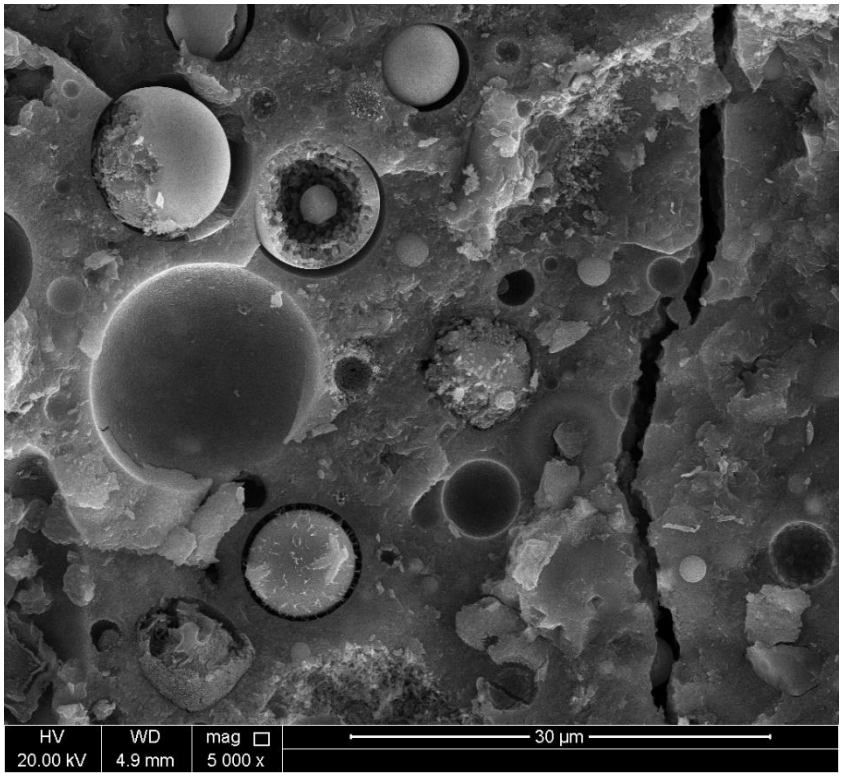

M2F1N1

fc = 54.3 MPa

5000x Mag.

Figure 31.SEM Images for GPM mix design M2F1N1

Figure 32 shows the SEM images for GPM mix design M3F1N1, which attained the highest compressive strength of all GPM mixes with a compressive strength of 63.9 MPa. It can be noted that the matrix is denser than both GPM mixes of M1F1N1 and M2F1N1. Further, there are less unreacted FA particles in the mix.

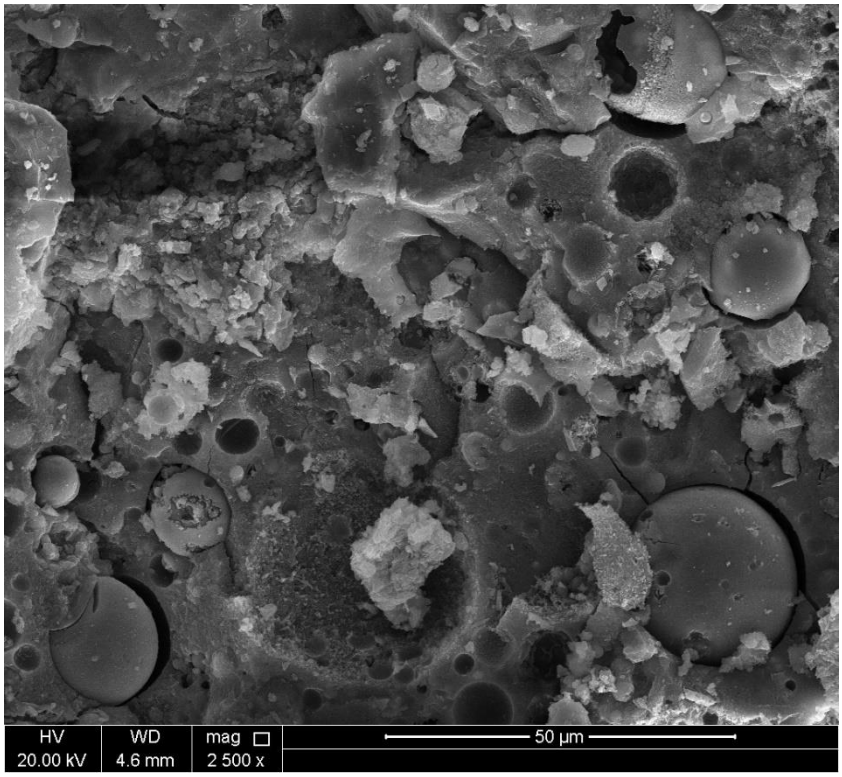

M3F1N1

fc = 63.9 MPa

2500x Mag.

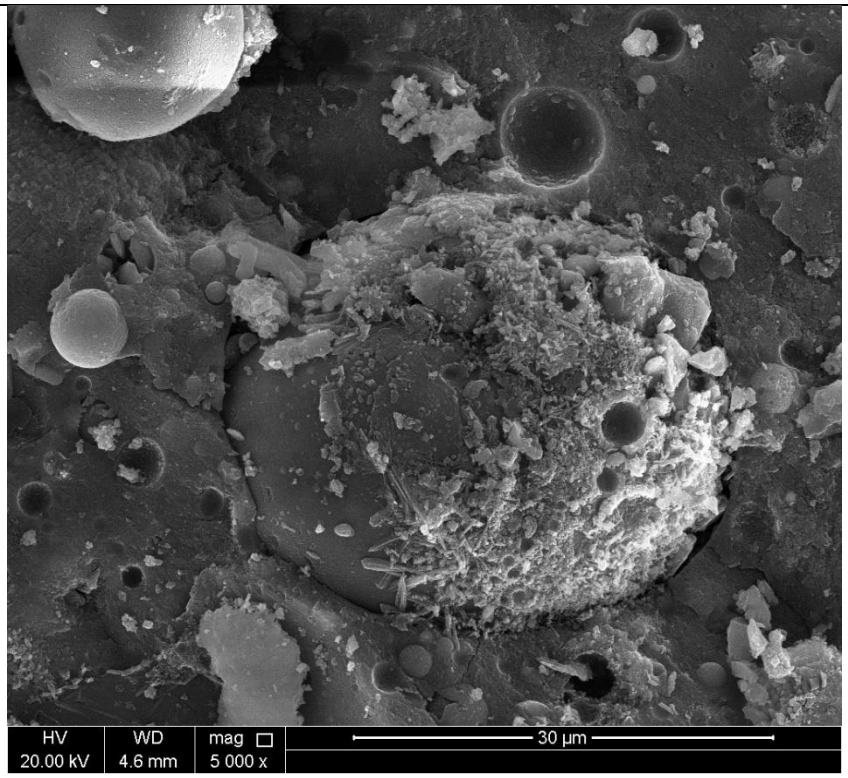

M3F1N1

fc = 63.9 MPa

5000x Mag.

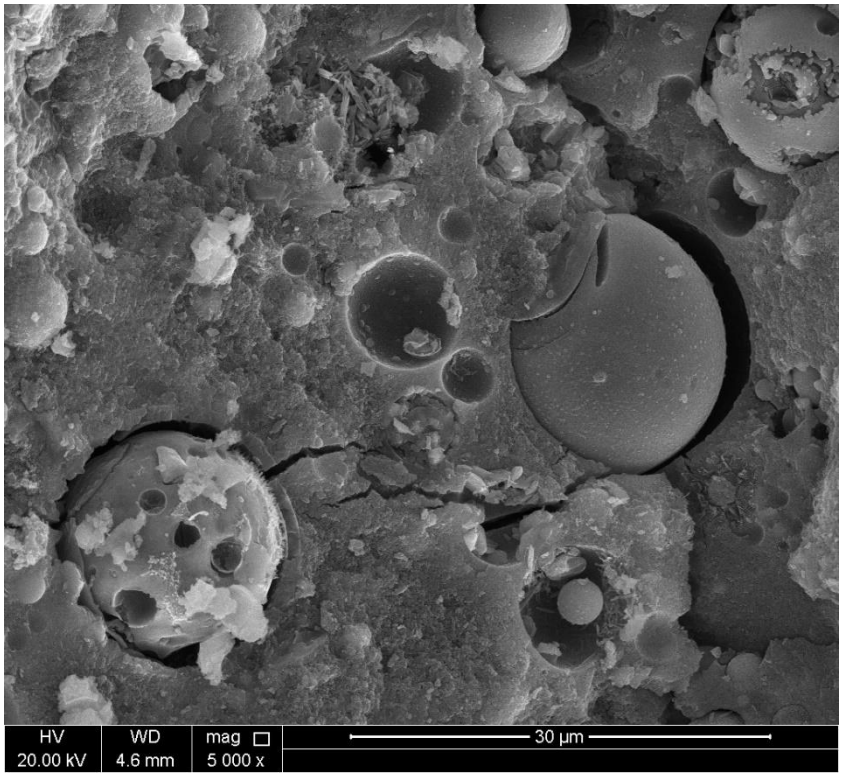

M3F1N1

fc = 63.9 MPa

5000x Mag.

Figure 32. SEM Images for GPM mix design M3F1N1

The effect of the molarity of the NaOH solution has been clearly observed through the SEM images. The higher the molarity of the NaOH solution the better the microstructure of the GPM as the amount of reacted FA particles increases, and the less pores the matrix becomes. These factors ultimately affect the compressive strength of GPM.

4.3.2 Effect of curing temperature

The effect of curing temperature on GPM specimens was investigated through SEM. GPM specimens cured at temperatures of 40, 80 and 120 ^{o}C and cured for a duration of 48 hrs. were tested. The compressive strength of GPM for the studied samples were 18.17, 39.8 and 36.10 MPa for GPM specimens at temperatures of 40, 80 and 120 ^{o}C, respectively.

Figure 33 shows the SEM images for GPM specimens cured at 40 ^{o}C for a duration of 48 hrs. It was noted that from the SEM images that there was a lot of unreacted FA particles and the existence of cracks in the polymerization matrix.

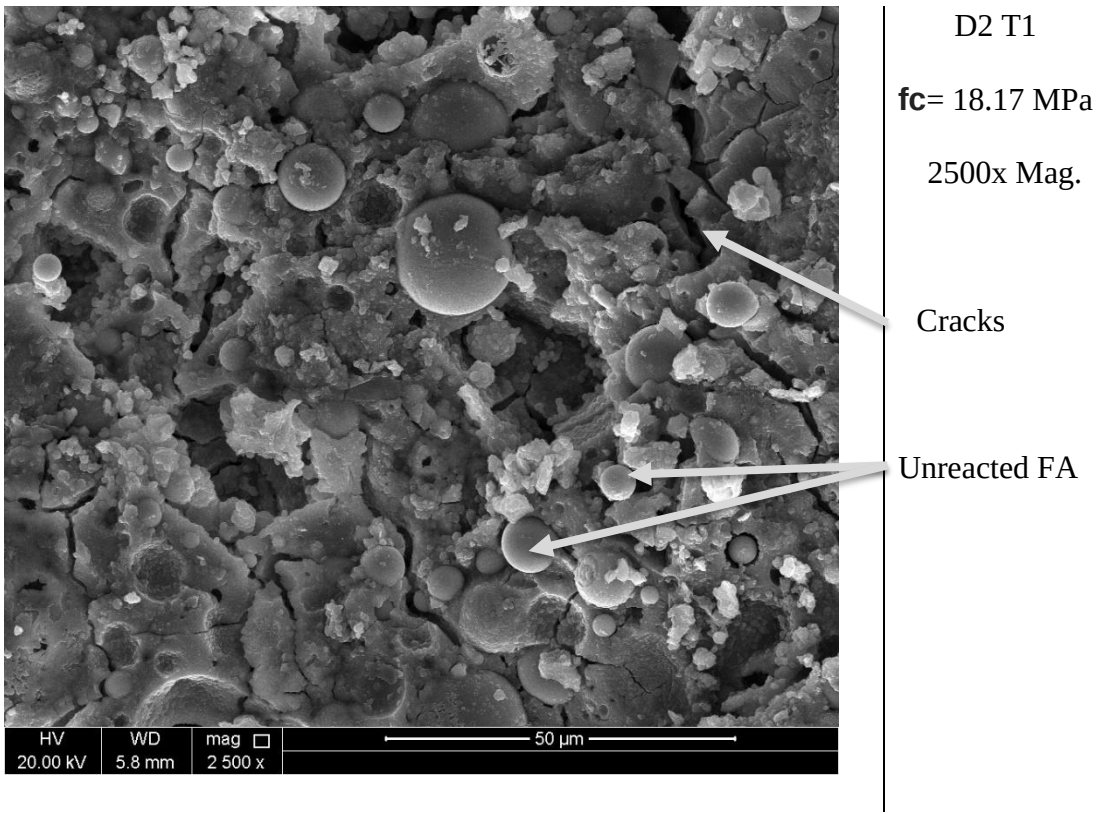

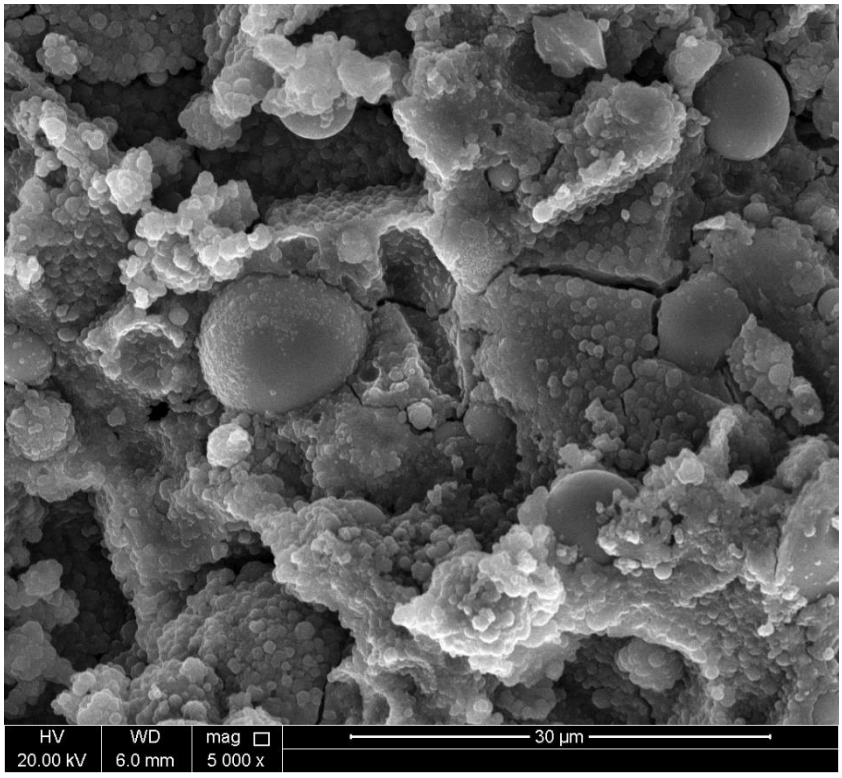

D2 T1

fc= 18.17 MPa

5000x Mag.

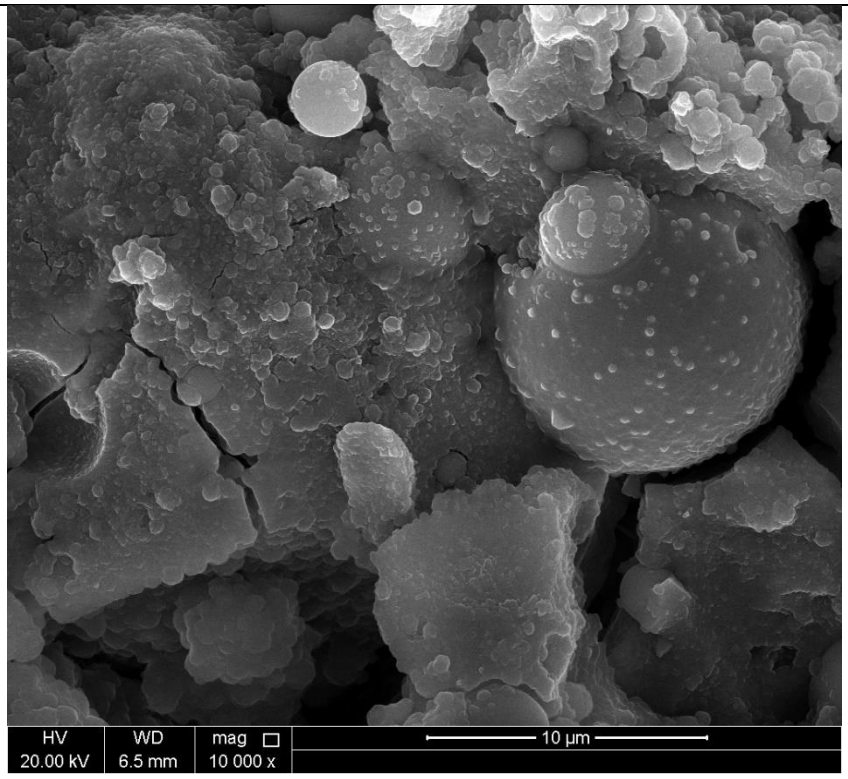

D2 T1

fc= 18.17 MPa

10000x Mag.

Figure 33.SEM Images for GPM mix design D2T1

For GPM specimens cured at 80 ^{o}C the SEM images at three magnification is shown in Figure 34. It can be observed that for GPM specimens cured at 80 ^{o}C, the dense polymerization matrix with most of FA particles reacted and covered by the polymerization matrix. Further, it was noted that there are less crack in the matrix compared to GPM specimens cured at 40 ^{o}C.

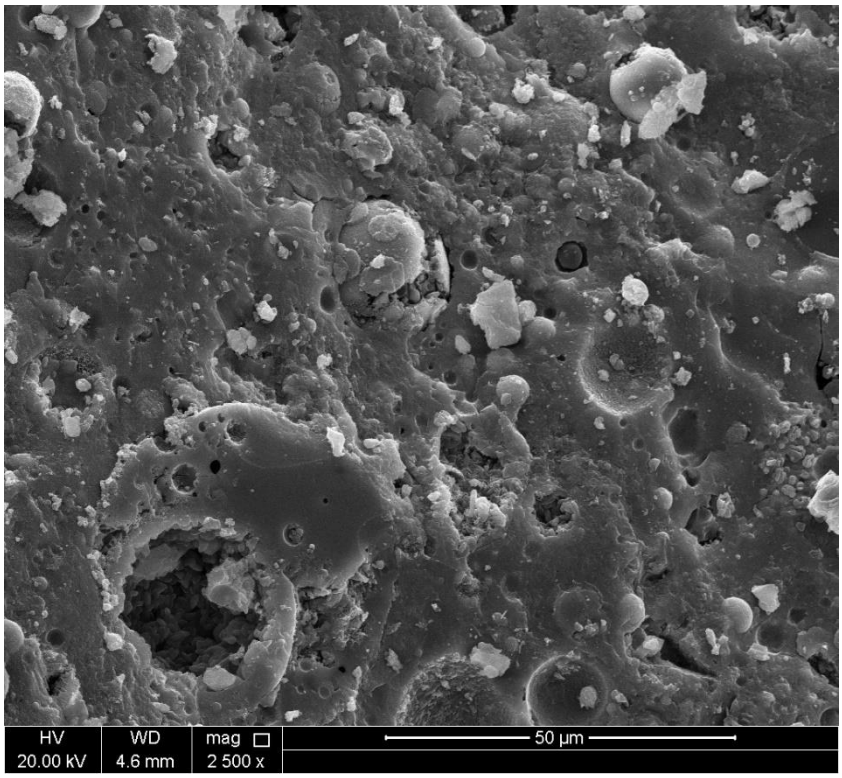

D2 T2

fc= 39.8 MPa

2500x Mag.

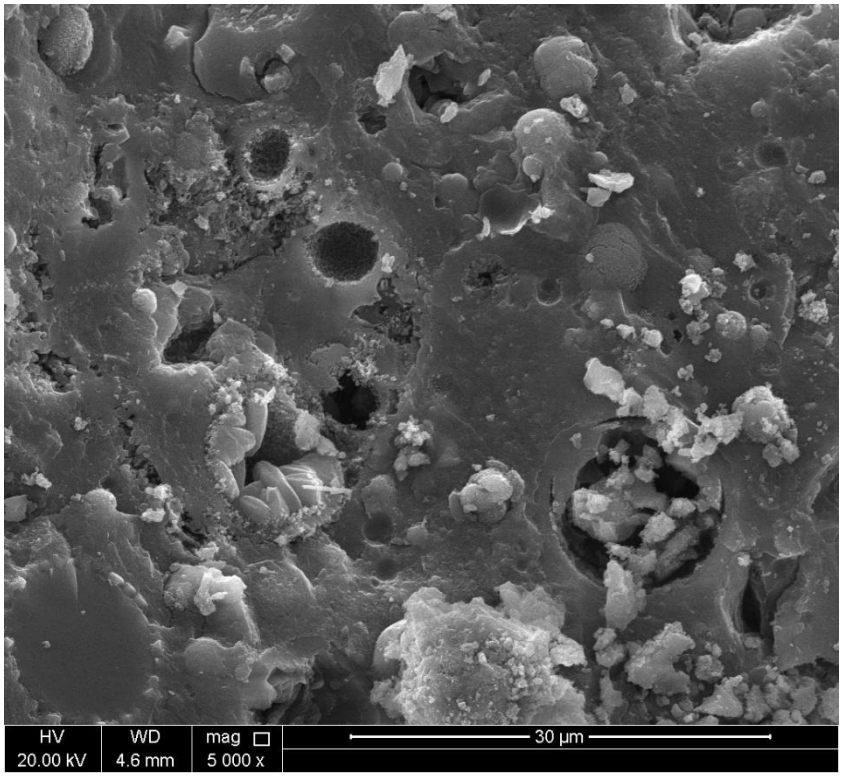

D2 T2

fc= 39.8 MPa

5000x Mag.

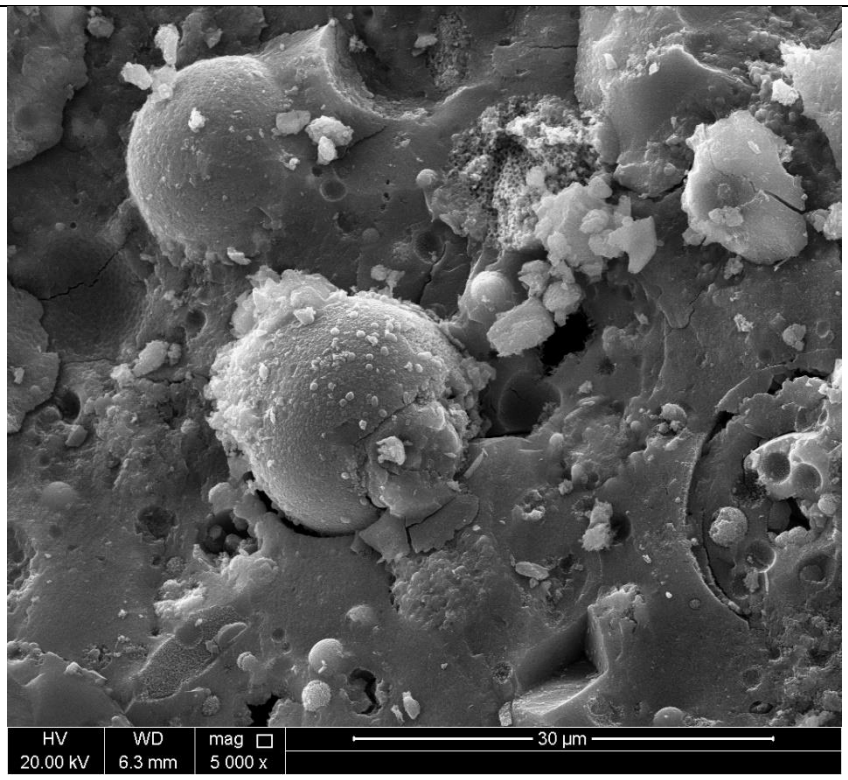

D2 T2

fc= 39.8 MPa

5000x Mag.

Figure 34. SEM Images for GPM mix design D2T2

For GPM specimens cured at 120 ºC the SEM images are shown in Figure 35. It can be observed from the SEM images that the polymerization matrix has needle shape, which can be related to the effect of high temperature curing. Further, it was observed that there were some unreacted particles of FA.

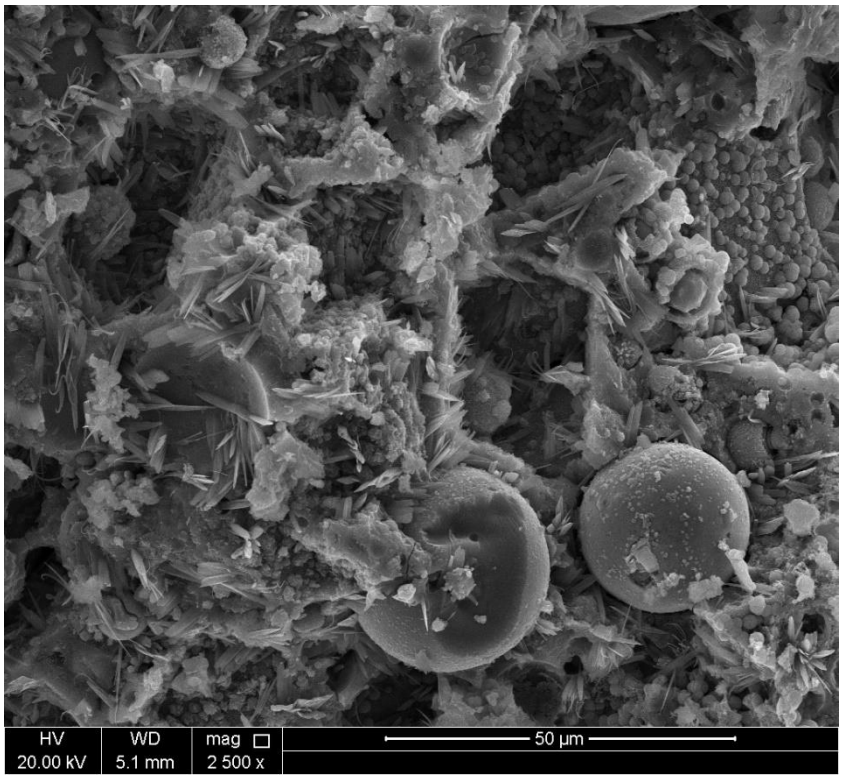

D2 T3

fc= 36.10 MPa

2500x Mag.

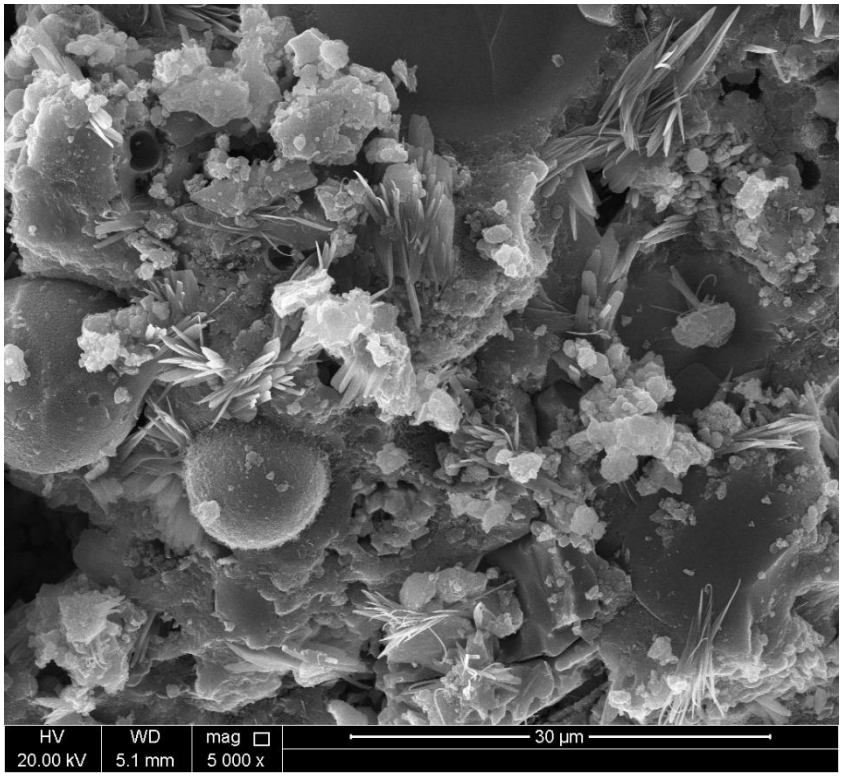

D2 T3

fc= 36.10 MPa

5000x Mag.

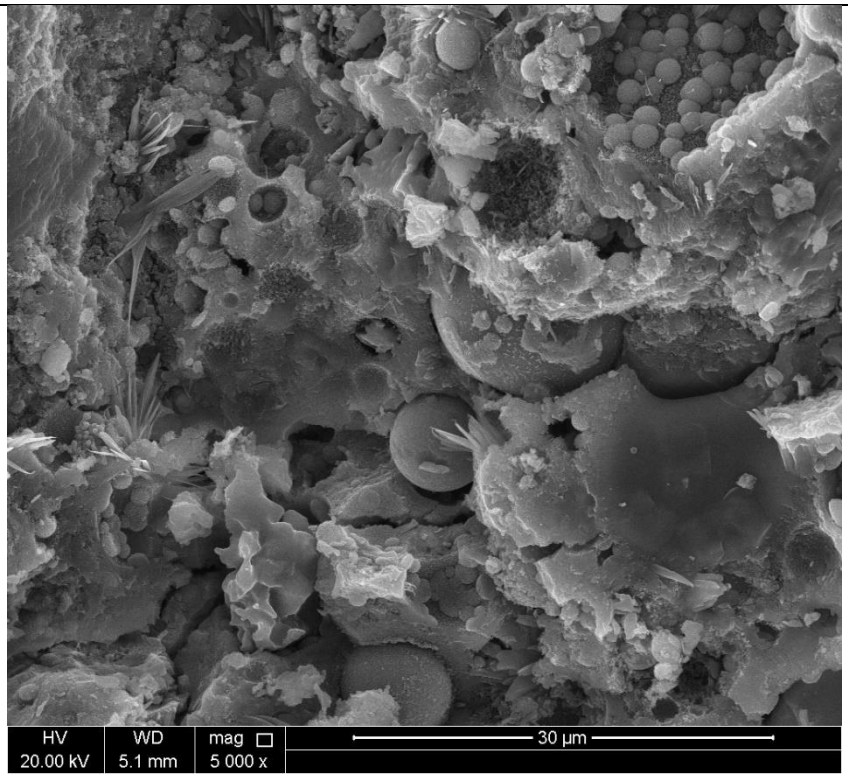

D2 T3

fc= 36.10 MPa

5000x Mag.

Figure 35. SEM Images for GPM mix design D2T3

The effect of heat curing with different temperatures is clearly observed in the SEM images. It can affect the polymerization matrix and the shape of the polymerization products. Further, it can be observed that as the temperature increases GPM becomes denser with less cracks and voids.

4.3.3 Effect of Activator solution

The effect of activating GPM with NaOH solution only was investigated through SEM images as shown in Figure 36. The compressive strength for GPM specimen activated only with NaOH solution attained a compressive strength of 18.4 MPa. It was observed that the polymerization matrix was full of thin NaOH needle shaped crystals, as well as a lot of unreacted FA particles. These needles were different from the polymerization products found in sample D2T3 as they were very thin and spread in all GPM specimen. It was mainly formed due to the excess of OH- ions from the sodium hydroxide solution.

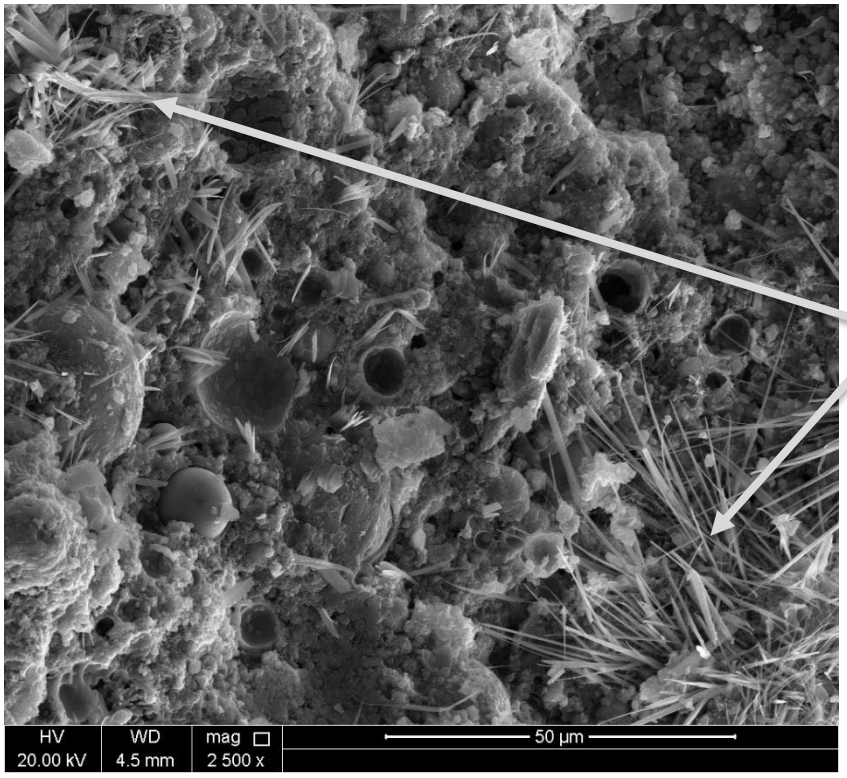

NaOH only

fc= 18.4 MPa

2500x Mag.

NaOH crystals (needles)

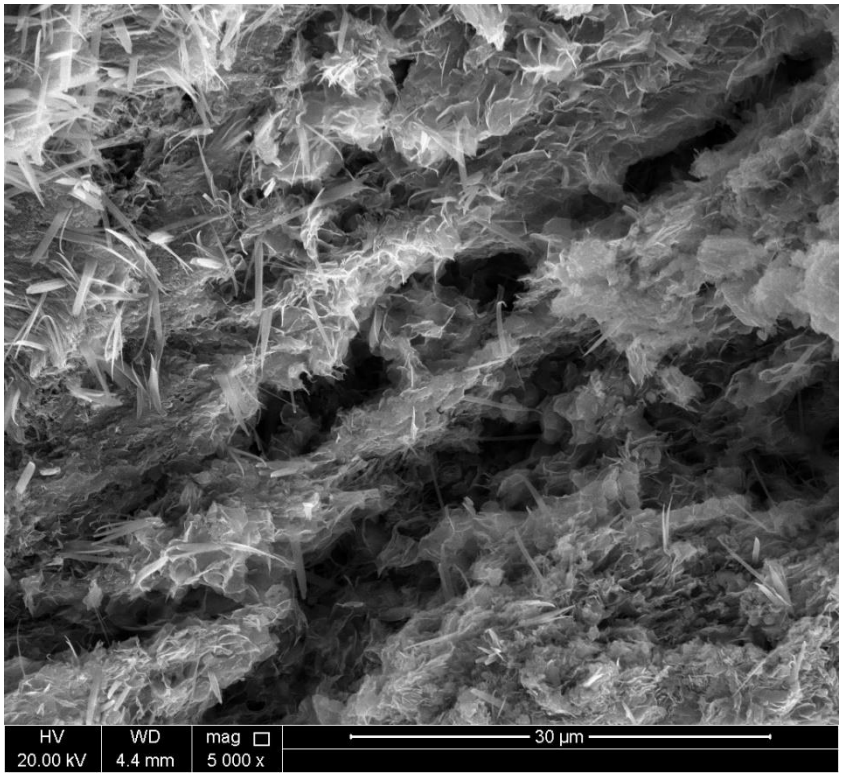

NaOH only

fc= 18.4 MPa

5000x Mag.

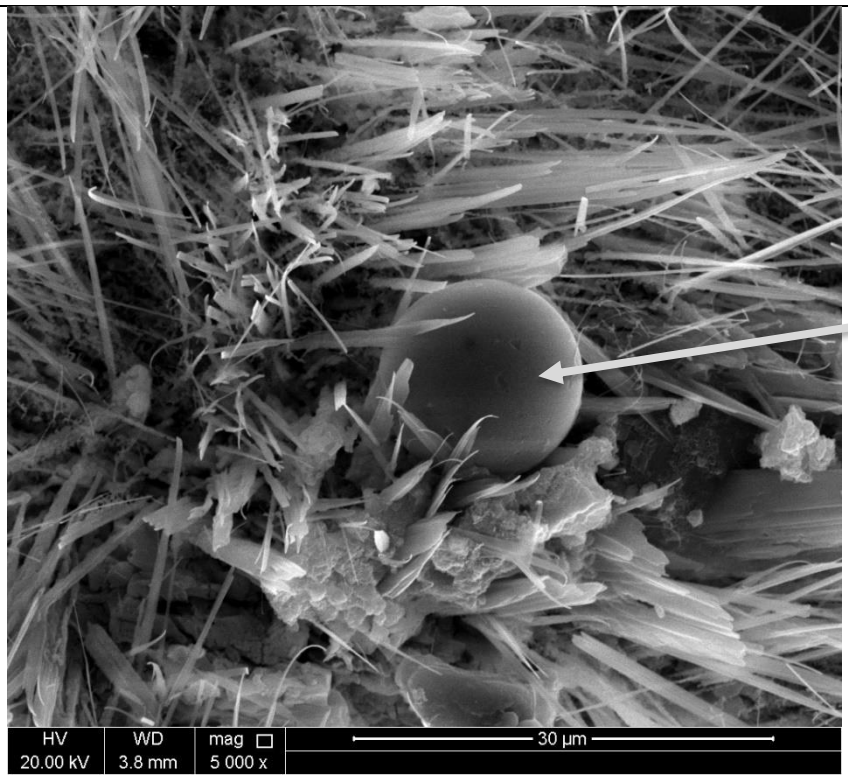

NaOH only

fc= 18.4 MPa

5000x Mag.

Unreacted FA

Figure 36.SEM Images for GPM mix design NaOH only

The effect of Molarity of NaOH activator solution, heat curing and the absence of sodium silicate solution were investigated through SEM images. It can be highlighted

that the molarity of the activator solution contributes to the development of the polymerization products and the internal structure of GPM. Further it can be observed how different curing temperature affects the shape of the polymerization products, and the amount of reacted FA particles. Moreover, it was clear how the absence of sodium silicate solution adversely affected the compressive strength and the internal structure of the GPM specimens. Similar observations of the microstructure of GPM were reported by multiple authors [1], [72]–[74].

4.4 X-Ray Diffraction Analysis (XRD)

The XRD analysis was conducted on the same GPM specimens investigated in the SEM to determine the qualitative composition of the compounds existing in different GPM specimens. Total of seven different GPM mix designs were investigated in this study, which is aimed to study the effect of the molarity of NaOH solution, the effect of the curing temperatures and the effect of the presence of sodium silicate solution. The procedure of the experimental work is mentioned in Chapter 3. The peaks found from the XRD graphs indicates the prominence of the polymerization products in the microstructure.

4.4.1 Effect of molarity

The effect of the molarity was investigated by conducting XRD analysis on GPM specimens M1F1N1, M2F1N1 and M3F1N1. Figure 37 shows the XRD results for GPM specimens activated with different molarities of the activator solution. It can be noted that the peak for mix design M3F1N1 was the highest which indicates high presence of Quartz (Q) and some presence of Hematite and Mullite (M). The XRD results conforms with the SEM images and compressive strength results.

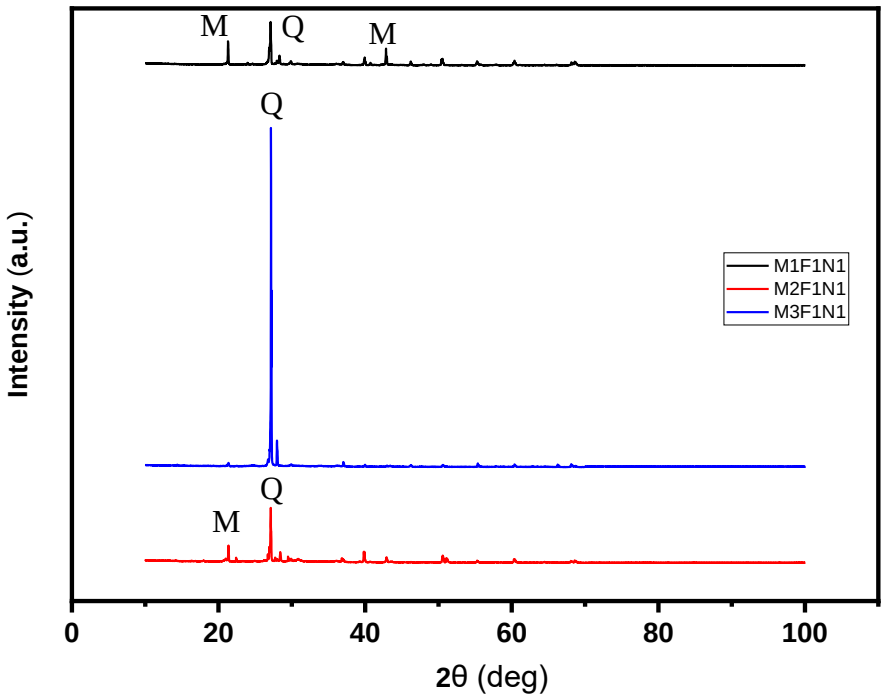

Figure 37. XRD for GPM specimens at different molarities

4.4.2 Effect of temperature

The effect of temperature was investigated using XRD analysis for GPM samples cured for a duration of 48 hrs. and as shown in Figure 38. It can be noted that for D2T2 the peaks of quartz and were higher and existing in different phases.

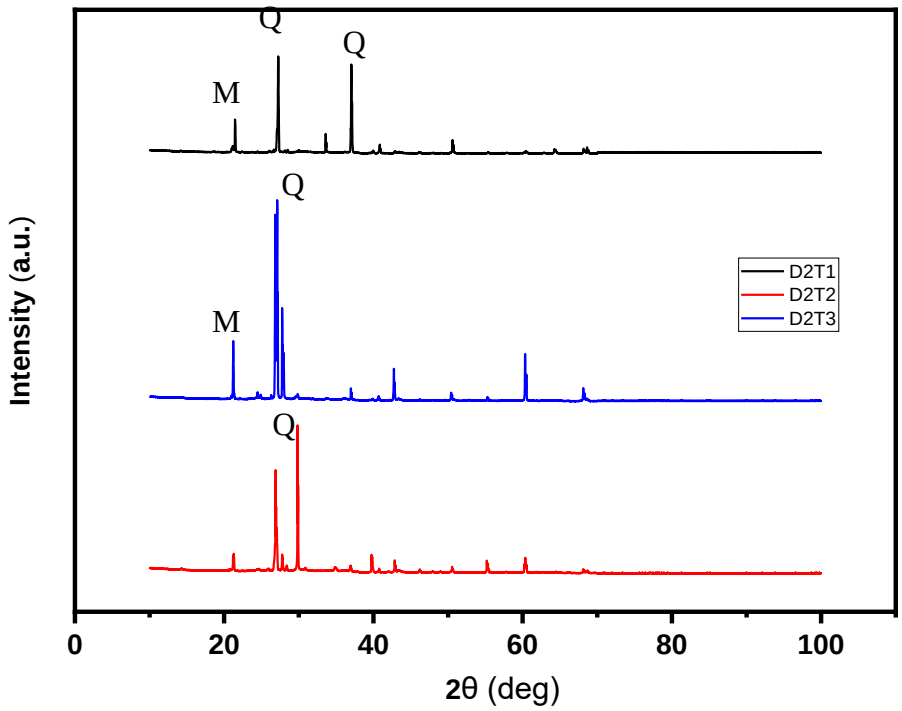

Figure 38. XRD of GPM specimens at different curing temperatures

4.5 Energy-Dispersive X-ray Spectroscopy (EDX)

The EDX analysis is used to provide a semi-quantitative of the elements existing in the GPM mixes [45]. It can be noted that FA supplying for (Si and Al) elements, and the activator solution supplies (Na). The SEM results were confirmed using EDX analysis that was conducted on three locations of the specimen, and an average of three locations is reported in Table 10. The same geopolymer specimens that was investigated using the SEM are used in the EDX analysis.

It can be noted that the percentage of Si and Al in GPM mix design of M3F1N1 is the highest among the elements of interest (Si and Al), which indicates high geopolymerization products [75], which is confirmed by both the SEM analysis and the compressive strength. On the contrary, the lowest weight percentage of Si and Al

supplied by FA was for GPM mix design activated by NaOH solution only. Further, it can be noted the high sodium content in the NaOH specimen.

Table 10. EDS results of GPM specimens

Mix Design	C	O	Na	Mg	Al	Si	K	Ca	Fe
NaOH	31.40	43.48	16.92	0.69	2.04	3.71	0.18	0.84	0.73
M1F1N1	28.44	42.32	6.95	1.45	4.99	11.28	0.58	2.41	1.59
M2F1N1	36.01	39.96	5.15	1.45	4.72	8.70	0.35	1.69	1.98
M3F1N1	23.47	43.79	7.18	1.61	6.13	12.01	0.47	2.72	2.63
D2T1	42.48	37.27	6.37	1.16	2.97	6.49	0.29	1.85	1.12
D2T2	25.98	43.42	7.09	2.62	4.43	10.67	0.42	3.21	2.17
D2T3	25.90	43.53	9.44	1.70	3.24	9.27	0.00	2.29	4.62

4.6 Cost Analysis

The wide adoption of using geopolymer mortar in the construction industry is not solely dependent on the positive environmental impact of producing geopolymer construction material, but also highly dependent on the financial competitiveness of these materials compared to ordinary Portland cement. Therefore, a brief cost analysis study is conducted to compare the costs resulted from producing $1m^3$ of cement mortar (CM) versus the cost required to produce $1m^3$ of geopolymer mortar. The optimum mix design of GPM M3F1N1 which attained the highest compressive strength was used to conduct the cost analysis study. The materials required to produce 1 m^3 of both cement mortar and geopolymer mortar are summarized in Table 11.

Table 11. Mix design per $1m^3$ of geopolmer and cement mortar

Mix design ID	Fly ash (Kg)	Sand (Kg)	NaOH solution (Kg)	Na2SiO3 solution (Kg)	Cement (Kg)	Water (Kg)
GPM	711.2	1955.5	213.3	213.3	N. A	N. A
CM	N. A	1943.3	N. A	N. A	706.7	342.7
Unit Price (QAR)	0.4	0.555	5	4	0.26	0.0054

The unit price for the materials are based on locally available suppliers in Qatar. The cost of producing 1 m^3 of GPM is 3,290 QAR compared to 1,264 QAR of producing cement mortar. The cost of producing GPM is higher than the cost of producing ordinary Portland cement mortar by a factor of 2.6. The significance price difference is due to the use of the activator solutions in GPM. Even though, the cost of producing GPM is higher than cement mortar which is hindering the wide spread of using GPM in civil engineering applications. The high early compressive strength of GPM is considered as the main advantage of using GPM over OPC cement mortar.

CHAPTER 5: CONCLUSION AND RECOMMENDATIONS

This thesis introduced an experimental study on the factors affecting the mechanical properties of geopolymer mortar using fly ash. Total of 162 GPM cubes were casted to investigate the effect of molarity of NaOH solution, fluid to binder ratio, Na2SiO3/NaOH and curing conditions as temperature and duration. The compressive strength and flow table test were conducted to assess the mechanical properties rheology of GPM. A microstructural analysis was conducted using scanning electron microscopy (SEM), X-ray diffraction analysis and Energy dispersive X-ray spectroscopy to study the development of the geopolymerization products. The main conclusions of this study can be summarized as follows:

- It is possible to obtain a very high early compressive strength of 63.9 MPa from GPM specimen made of fly ash class F, activated by 16 M NaOH solution and sodium silicate to sodium hydroxide ratio of one.
- The effect of molarity of NaOH solution varied across different fluid to binder ratios:
    - For fluid to binder ratio of 0.60, 16 M NaOH solution resulted in the highest compressive strength for all GPM and it was above 61.8 MPa.
    - For fluid to binder ratio of 0.65, the effect of molarity varied across different sodium silicate to sodium hydroxide ratios. However, all GPM specimens obtained a compressive strength above 45.1 MPa
    - For fluid to binder ratio of 0.70, the compressive strength was higher for molarities of 12 M and 14 M than 16 M NaOH solution.
- The effect of fluid to binder ratios on the compressive strength of GPM had little

variations across different sodium silicate to sodium hydroxide ratios.

  - For GPM specimens activated with 12 M NaOH hydroxide solution the compressive strength had similar trend for sodium silicate to sodium hydroxide ratio of 1 and 1.5, with the maximum compressive strength obtained by F/B ratio of 0.65. For sodium silicate to sodium hydroxide ratios of 2 and 2.5 the compressive strength had the same trend, with maximum strength at F/B ratio of 0.60 and minimum at F/B ratio of 0.70.
  - For GPM specimens activated with 14 M and 16 M of NaOH hydroxide solution the compressive strength had similar trend across all ratios of sodium silicate to sodium hydroxide.

- The effect of sodium silicate to sodium hydroxide ratios on the compressive strength of GPM specimens varied across different fluid to binder ratio and with different molarities.
- Heat curing is necessary to achieve early compressive strength for GPM, with optimum curing temperature of 80 ^{o}C and curing duration of 24 hrs.
- GPM gains strength with age for both heat curing and room temperature curing, the rate of gaining the strength in case of heat curing is rapid for the first 24 hrs. then slow development of the strength over time occur. For room temperature curing the gain in compressive strength is very low over time.
- GPM specimens can be cured at lower temperatures for longer periods to achieve adequate compressive strengths. Higher curing temperature for shorter periods lead to increase in the early strength of GPM.
- Geopolymer activated by Sodium hydroxide only has very low compressive strength compared to that achieved by made of both sodium hydroxide and sodium silicate, which is confirmed by SEM results.

5.1 Recommendations and future work

The factors affecting the mechanical properties of GPM were comprehensively covered. The optimum mix design of GPM made of fly ash class F is activated with 16M NaOH solution and sodium silicate solution at a ratio of one. The curing conditions should be adjusted to 80 ^{o}C and for a duration of 24 hrs.

Future work can include investigating the feasibility of producing high strength geopolymer binder cured at room temperature. In addition, utilization of geopolymer concrete in civil engineering applications to replace OPC concrete is highly recommended to study.

REFERENCES

[1] C. Ng, U. J. Alengaram, L. S. Wong, K. H. Mo, M. Z. Jumaat, and S. Ramesh, "A review on microstructural study and compressive strength of geopolymer mortar, paste and concrete," *Constr. Build. Mater.*, vol. 186, pp. 550–576, 2018.

[2] B. Singh, G. Ishwarya, M. Gupta, and S. K. Bhattacharyya, "Geopolymer concrete: A review of some recent developments," *Constr. Build. Mater.*, vol. 85, pp. 78–90, 2015.

[3] M. F. Alnahhal, U. J. Alengaram, and M. Z. Jumaat, "Evaluation of Industrial By-Products as Sustainable Pozzolanic Materials in Recycled Aggregate Concrete," 2017.

[4] U. Rattanasak and P. Chindaprasirt, "Influence of NaOH solution on the synthesis of fly ash geopolymer," *Miner. Eng.*, vol. 22, no. 12, pp. 1073–1078, 2009.

[5] E. B. Görür, O. Karahan, C. Bilim, S. Ilkentapar, and E. Luga, "Very high strength (120 MPa) class F fly ash geopolymer mortar activated at different NaOH amount , heat curing temperature and heat curing duration," vol. 96, pp. 673–678, 2015.

[6] M. R. Irshidat, Y. A. Abdel-Jawad, and R. Al-Sughayer, "Feasibility of producing sustainable geopolymer composites made of locally available natural pozzolan," *J. Mater. Cycles Waste Manag.*, 2018.

[7] H. . S. cement Kühl, "and process of making the same," *U.S. Pat.*, vol. 900, p. 939, 1908.

[8] A. O. Purdon, "The action af alkalis on blast furnace slag," *J. Soc. Chem. Ind.*, 1940.

[9] J. Davidovits, "Geopolymers," *J. Therm. Anal.*, 1991.

[10] I. Beleña, M. J. L. Tendero, E. M. Tamayo, and D. Vie, “Study and obtimizing of the reaction parametres for geopolymeric material manufacture,” *Bol. la Soc. Esp. Ceram. y Vidr.*, 2004.

[11] U.S. Geological Survey, “Mineral Commodity Summaries 2015 Mineral Commodity Summaries 2015,” *US Geol. Surv.*, 2015.

[12] P. C. Aïtcin, “Cements of yesterday and today - concrete of tomorrow,” *Cement and Concrete Research*. 2000.

[13] L. J. Hanle, “CO 2 Emissions Profile of the U . S . Cement Industry,” *US Environ. Prot. Agency*, 2004.

[14] R. Maddalena, J. J. Roberts, and A. Hamilton, “Can Portland cement be replaced by low-carbon alternative materials? A study on the thermal properties and carbon emissions of innovative cements,” *J. Clean. Prod.*, 2018.

[15] J. S. Damtoft, J. Lukasik, D. Herfort, D. Sorrentino, and E. M. Gartner, “Sustainable development and climate change initiatives,” *Cem. Concr. Res.*, 2008.

[16] M. C. G. Juenger, F. Winnefeld, J. L. Provis, and J. H. Ideker, “Advances in alternative cementitious binders,” *Cement and Concrete Research*. 2011.

[17] J. Davidovits, “Geopolymers - Inorganic polymeric new materials,” *J. Therm. Anal.*, vol. 37, no. 8, pp. 1633–1656, Aug. 1991.

[18] D. M. J. Sumajouw, D. Hardjito, S. E. Wallah, B. V Rangan, and others, “Behaviour and strength of reinforced fly ash-based geopolymer concrete beams,” in *Australian Structural Engineering Conference 2005*, 2005.

[19] X. Hua, J. L. Provis, J. S. J. Van Deventer, and P. V. Krivenko, “Characterization of Aged Slag Concretes,” *ACI Mater. J.*, 2008.

[20] H. Uchikawa and S. Hanehara, *Waste Materials Used in Concrete*

Manufacturing. 1996.

[21] K. Zerfu and J. J. Ekaputri, "Review on alkali-activated fly ash based geopolymer concrete," in *Materials Science Forum*, 2016.

[22] Y. Park, A. Abolmaali, Y. H. Kim, and M. Ghahremannejad, "Compressive strength of fly ash-based geopolymer concrete with crumb rubber partially replacing sand," *Constr. Build. Mater.*, 2016.

[23] L. K. Turner and F. G. Collins, "Carbon dioxide equivalent (CO2-e) emissions: A comparison between geopolymer and OPC cement concrete," *Constr. Build. Mater.*, 2013.

[24] D. Bondar, C. J. Lynsdale, N. B. Milestone, N. Hassani, and A. A. Ramezanianpour, "Effect of adding mineral additives to alkali-activated natural pozzolan paste," *Constr. Build*, vol. 25, no. 6, pp. 2906–2910, 2011.

[25] G. Nagalia, Y. Park, A. Abolmaali, and P. Aswath, "Compressive strength and microstructural properties of fly ash-based geopolymer concrete," *J. Mater. Civ. Eng.*, 2016.

[26] M. S. Reddy, P. Dinakar, and B. H. Rao, "A review of the influence of source material's oxide composition on the compressive strength of geopolymer concrete," *Microporous and Mesoporous Materials*. 2016.

[27] P. Chindaprasirt, T. Chareerat, S. Hatanaka, and T. Cao, "High-Strength Geopolymer Using Fine High-Calcium Fly Ash," *J. Mater. Civ. Eng.*, 2011.

[28] T. Silverstrim, J. Martin, and H. Rostami, "Geopolymeric fly ash cement," *Geopolymere '99*, 1999.

[29] D. Hardjito, S. E. Wallah, D. M. J. Sumajouw, and B. V. Rangan, "On the Development of Fly Ash-based Geopolymer Concrete_Djwantoro Hardjito dkk," no. 101, pp. 467–472, 2005.

[30] A. M. Mustafa Al Bakri, H. Kamarudin, A. K. Omar, M. N. Norazian, C. M. Ruzaidi, and A. R. Rafiza, “The effect of alkaline activator ratio on the compressive strength of fly ash-based geopolymers,” *Aust. J. Basic Appl. Sci.*, 2011.

[31] D. Panias, I. P. Giannopoulou, and T. Perraki, “Effect of synthesis parameters on the mechanical properties of fly ash-based geopolymers,” *Colloids Surfaces A Physicochem. Eng. Asp.*, 2007.

[32] A. M. Mustafa Al Bakria, H. Kamarudin, M. Bin Hussain, I. Khairul Nizar, Y. Zarina, and A. R. Rafiza, “The effect of curing temperature on physical and chemical properties of geopolymers,” in *Physics Procedia*, 2011.

[33] J. Temuujin, R. P. Williams, and A. van Riessen, “Effect of mechanical activation of fly ash on the properties of geopolymer cured at ambient temperature,” *J. Mater. Process. Technol.*, 2009.

[34] M. Kaur, J. Singh, and M. Kaur, “Synthesis of fly ash based geopolymer mortar considering different concentrations and combinations of alkaline activator solution,” *Ceram. Int.*, 2018.

[35] B. H. Mo, H. Zhu, X. M. Cui, Y. He, and S. Y. Gong, “Effect of curing temperature on geopolymerization of metakaolin-based geopolymers,” *Appl. Clay Sci.*, 2014.

[36] M. S. Muñiz-Villarreal *et al.*, “The effect of temperature on the geopolymerization process of a metakaolin-based geopolymer,” *Mater. Lett.*, 2011.

[37] C. Y. Heah *et al.*, “Effect of curing profile on kaolin-based geopolymers,” in *Physics Procedia*, 2011.

[38] Sindhunata, J. S. J. Van Deventer, G. C. Lukey, and H. Xu, “Effect of curing

temperature and silicate concentration on fly-ash-based geopolymerization," *Ind. Eng. Chem. Res.*, 2006.

[39] P. Rovnaník, "Effect of curing temperature on the development of hard structure of metakaolin-based geopolymer," *Constr. Build. Mater.*, 2010.

[40] G. Görhan and G. Kürklü, "The influence of the NaOH solution on the properties of the fly ash-based geopolymer mortar cured at different temperatures," *Compos. Part B Eng.*, 2014.

[41] C. D. Atiş, E. B. Görür, O. Karahan, C. Bilim, S. Ilkentapar, and E. Luga, "Very high strength (120 MPa) class F fly ash geopolymer mortar activated at different NaOH amount, heat curing temperature and heat curing duration," *Constr. Build. Mater.*, 2015.

[42] J. Xie and O. Kayali, "Effect of initial water content and curing moisture conditions on the development of fly ash-based geopolymers in heat and ambient temperature," *Constr. Build. Mater.*, 2014.

[43] A. Karthik, K. Sudalaimani, and C. T. Vijaya Kumar, "Investigation on mechanical properties of fly ash-ground granulated blast furnace slag based self curing bio-geopolymer concrete," *Constr. Build. Mater.*, vol. 149, pp. 338–349, 2017.

[44] A. Narayanan and P. Shanmugasundaram, "An Experimental Investigation on Flyash-based Geopolymer Mortar under different curing regime for Thermal Analysis," *Energy Build.*, 2017.

[45] M. H. Al-Majidi, A. Lampropoulos, A. Cundy, and S. Meikle, "Development of geopolymer mortar under ambient temperature for in situ applications," *Constr. Build. Mater.*, 2016.

[46] ASTM C618-17a, "Standard specification for coal fly ash and raw or calcined

natural pozzolan for use in concrete," *Annu. B. ASTM Stand.*, 2017.

[47] ASTM C 311-04, "Standard Test Methods for Sampling and Testing Fly Ash or Natural Pozzolans for Use in Portland-Cement Concrete.," *Annu. B. ASTM Stand.*, 2005.

[48] ASTM C188-09, "Standard Test Method for Density of Hydraulic Cement," *ASTM Int.*, 2009.

[49] ASTM Standard C778, "Standard Specification for Standard Sand," 2017.

[50] ASTM C109, "Standard Test Method for Compressive Strength of Hydraulic Cement Mortars," *ASTM Int. West Conshohocken*, 2000.

[51] ASTM Standard C109, "Standard Test Method for Compressive Strength of Hydraulic Cement Mortars (Using 2-in. or [50-mm] Cube Specimens)," pp. 1–10, 2019.

[52] ASTM, "C1437 - Standard test method for flow of hydraulic cement mortar," 2013.

[53] ASTM Committee C09.65, "ASTM C1723-10 Examination of Hardened Concrete Using Scanning Electron Microscopy," in *Annual Book of ASTM Standards Volume 04.02*, 2010.

[54] ASTM C1365, "Standard Test Method for Determination of the Proportion of Phases in Portland Cement and Portland-Cement Clinker Using X-Ray Powder Diffraction Analysis," *Am. Soc. Test. Mater.*, 2006.

[55] Astm, "ASTM E1508: Standard Guide for Quantitative Analysis by Energy-Dispersive Spectroscopy," *ASTM Stand.*, 2012.

[56] C. D. Budh and N. R. Warhade, "Effect of molarity on compressive strength of geopolymer mortar," *Int. J. Civ. Eng. Res.*, 2014.

[57] C. K. Madheswaran, G. Gnanasundar, and N. Gopalakrishnan, "Effect of

molarity in geopolymer concrete," *Int. J. Civ. Struct. Eng.*, 2013.

[58] S. V Patankar, S. S. Jamkar, and Y. M. Ghugal, "Effect of Water-To-Geopolymer Binder Ratio on the Production of Fly Ash Based Geopolymer Concrete," *Int. J. Adv. Technol. Civ. Eng.*, 2013.

[59] B. Nematollahi and J. Sanjayan, "Effect of different superplasticizers and activator combinations on workability and strength of fly ash based geopolymer," *Mater. Des.*, 2014.

[60] P. S. Deb, P. Nath, and P. K. Sarker, "The effects of ground granulated blast-furnace slag blending with fly ash and activator content on the workability and strength properties of geopolymer concrete cured at ambient temperature," *Mater. Des.*, 2014.

[61] S. İlkentapar, C. D. Atiş, O. Karahan, and E. B. Görür Avşaroğlu, "Influence of duration of heat curing and extra rest period after heat curing on the strength and transport characteristic of alkali activated class F fly ash geopolymer mortar," *Constr. Build. Mater.*, 2017.

[62] M. T. Junaid, "PERFORMANCE OF GEOPOLYMER CONCRETE AT ELEVATED TEMPERATURES," The University of New South Wales, 2015.

[63] Y. M. Liew *et al.*, "Effect of curing regimes on metakaolin geopolymer pastes produced from geopolymer powder," in *Advanced Materials Research*, 2013.

[64] P. U, P. Rao S, and M. Raju P, "The effect of age on Alkali-Activated Geopolymer mortar at ambient temperature," *Int. J. Civ. Eng.*, 2016.

[65] B. Nematollahi, J. Sanjayan, and F. U. A. Shaikh, "Synthesis of heat and ambient cured one-part geopolymer mixes with different grades of sodium silicate," *Ceram. Int.*, 2015.

[66] P. Nath and P. . . Sarker, "Geopolymer concrete for ambient curing condition,"

in *Australasian Structural Engineering Conference 2012: The past, present and future of Structural Engineering*, 2012.

[67] ASTM Standard C230, "Standard Specification for Flow Table for Use in Tests of Hydraulic Cement 1," pp. 1–6, 2014.

[68] P. Zhang, Y. Zheng, K. Wang, and J. Zhang, "A review on properties of fresh and hardened geopolymer mortar," *Composites Part B: Engineering*. 2018.

[69] A. Sathonsaowaphak, P. Chindaprasirt, and K. Pimraksa, "Workability and strength of lignite bottom ash geopolymer mortar," *J. Hazard. Mater.*, 2009.

[70] P. Chindaprasirt, T. Chareerat, and V. Sirivivatnanon, "Workability and strength of coarse high calcium fly ash geopolymer," *Cem. Concr. Compos.*, 2007.

[71] S. Alehyen, M. El Achouri, and M. Taibi, "Characterization, microstructure and properties of fly ash-based geopolymer," *J. Mater. Environ. Sci.*, 2017.

[72] A. M. Izzat *et al.*, "Microstructural analysis of geopolymer and ordinary Portland cement mortar exposed to sulfuric acid," *Mater. Plast.*, 2013.

[73] R. Zejak, I. Nikolić, D. Blečić, V. Radmilović, and V. Radmilović, "Mechanical and microstructural properties of the fly-ash-based geopolymer paste and mortar," *Mater. Tehnol.*, 2013.

[74] M. Sumesh, U. J. Alengaram, M. Z. Jumaat, K. H. Mo, and M. F. Alnahhal, "Incorporation of nano-materials in cement composite and geopolymer based paste and mortar – A review," *Construction and Building Materials*. 2017.

[75] M. S. Morsy, S. H. Alsayed, Y. Al-Salloum, and T. Almusallam, "Effect of Sodium Silicate to Sodium Hydroxide Ratios on Strength and Microstructure of Fly Ash Geopolymer Binder," *Arab. J. Sci. Eng.*, 2014.